ANL-7499

Argonne National Laboratory

INELASTIC RESPONSE OF PRIMARY REACTOR CONTAINMENT TO HIGH-ENERGY EXCURSIONS

by

Gabriel Cinelli, Jr., Joseph Gvildys,
and Stanley H. Fistedis

The facilities of Argonne National Laboratory are owned by the United States Government. Under the terms of a contract (W-31-109-Eng-38) between the U. S. Atomic Energy Commission, Argonne Universities Association and The University of Chicago, the University employs the staff and operates the Laboratory in accordance with policies and programs formulated, approved and reviewed by the Association.

MEMBERS OF ARGONNE UNIVERSITIES ASSOCIATION

The University of Arizona	Kansas State University	The Ohio State University
Carnegie-Mellon University	The University of Kansas	Ohio University
Case Western Reserve University	Loyola University	The Pennsylvania State University
The University of Chicago	Marquette University	Purdue University
University of Cincinnati	Michigan State University	Saint Louis University
Illinois Institute of Technology	The University of Michigan	Southern Illinois University
University of Illinois	University of Minnesota	University of Texas
Indiana University	University of Missouri	Washington University
Iowa State University	Northwestern University	Wayne State University
The University of Iowa	University of Notre Dame	The University of Wisconsin

Printed in the United States of America
Available from
Clearinghouse for Federal Scientific and Technical Information
National Bureau of Standards, U. S. Department of Commerce
Springfield, Virginia 22151
Price: Printed Copy $3.00; Microfiche $0.65

ANL-7499
Reactor Technology

ARGONNE NATIONAL LABORATORY
9700 South Cass Avenue
Argonne, Illinois 60439

INELASTIC RESPONSE OF PRIMARY REACTOR CONTAINMENT TO HIGH-ENERGY EXCURSIONS

by

Gabriel Cinelli, Jr., Joseph Gvildys,
and Stanley H. Fistedis

Reactor Engineering Division

November 1969

TABLE OF CONTENTS

LIST OF FIGURES

INELASTIC RESPONSE OF PRIMARY REACTOR CONTAINMENT TO HIGH-ENERGY EXCURSIONS

by

Gabriel Cinelli, Jr., Joseph Gvildys,
and Stanley H. Fistedis

ABSTRACT

The inelastic response of primary containment to a high-energy axisymmetric excursion is found by numerical techniques. First, the equation of state for inelastic behavior is discussed. Then the basic conservation laws of mass, momentum, and energy are given in Eulerian coordinates. These equations are then transformed into Lagrangian coordinates and the finite-difference equations for numerical computation. Finally, the results of a sample problem calculation are given.

I. INTRODUCTION

Knowledge of the containment potential of a particular reactor design is essential in assessing the overall safety of a nuclear power plant concept. To determine this potential, the containment response to a prompt critical excursion must be analyzed. During such an excursion, a high-pressure (200-300 kb) shock wave is developed, which propagates through the primary containment, causing damage. Therefore, the goal of the Primary Containment Program at Argonne is to devise theoretical methods for determining the type and amount of damage done by the shock wave.

One of the questions that must be answered is: How does the material strength of the primary containment affect the progress of the shock wave? If the pressure is 100 kb or more, the approximation of the material to a fluid is valid, since the material shear strength is a few kilobars. Experiments with metals at 50 kb or below show that the wave-propagation velocity is greater than that given by hydrodynamic theory. Hence, material strength must be accounted for when the shock-wave pressure is less than 50 kb.

As the shock wave progresses through the primary containment, it strikes the blanket material, the coolant, the pressure vessel, the blast shield, and the biological shielding, in that order. Since the pressure is so high, the blanket material can be treated on a hydrodynamic basis, but, due

to the decay of the shock wave in the coolant, the pressure vessel must include the effect of material strength. Incorporation of material strength in the equation of motion requires that the equations be written in terms of the stress components. In this way, the material shear strength is included automatically.

The purpose of this report is the solution, by finite-difference methods, of axisymmetric wave propagation in compressible material with shear strength accounted for. Lagrangian grid representation is used. For this system, the motion of the medium is described with reference to a mesh attached to the material. This results in a limitation of the method when severe distortions of the original mesh take place. The program can be used with a fluid or elastic-perfectly-plastic solid. The polynomial equation of state is used for describing the hydrostatic component of the stresses.

The remainder of this report is divided into three parts. Section II describes the equation of state. Section III treats the equations of motion and discusses the finite-difference equations. Section IV gives the results of computer code calculations on a sample problem.

II. EQUATION OF STATE

The first requirement in the calculation of elastic-plastic flow is to formulate the equation of state. This equation must describe elastic, elastic-plastic, and hydrodynamic flow, and include appropriate yield criteria in the latter two regimes. The literature contains many complicated forms of equations of state; some are designed to aid the mathematics in the analytic solution of equations of motion. However, since numerical techniques will be considered here, the equations of motion are independent of any rheological equation of state, and any form may be used. The objective of the equation of state will be to provide a theoretical description applicable to a wide class of practical problems, but using simple idealizations of the outstanding features of the real phenomenon. The plastic state will be described by continuously adjusting the stresses such that the yield strength is not exceeded.

A. Elastic Region

We shall consider media having the same properties in all directions, i.e., isotropic media.

In x, y, z coordinates, the state of stress in a continuous medium is defined at a given point by six stress components: σ_x, σ_y, σ_z, τ_{yz}, τ_{zx}, and τ_{xy} (Ref. 1, p. 14). It is always possible to choose coordinate axes such that

the shear stress at a given point is zero, i.e., $\tau_{yz} = \tau_{zx} = \tau_{xy} = 0$ (Ref. 2, p. 215). Any three orthogonal axes yielding the above conditions are called the principal axes for the point considered. Stresses in the directions of the principal axis on surfaces normal to these axes are called principal stresses.

A perfectly elastic material is characterized by a linear relationship between stress and strain. Hooke's law is used to describe the stress resulting from the strain at this point. The strain results from a force that displaces particles in the media. Hooke's law, in terms of an incremental stress resulting from an incremental strain, may be written

$$\left.\begin{aligned} \dot{\sigma}_1 &= \lambda\frac{\dot{V}}{V} + 2\mu\dot{\epsilon}_1; \\ \dot{\sigma}_2 &= \lambda\frac{\dot{V}}{V} + 2\mu\dot{\epsilon}_2; \\ \dot{\sigma}_3 &= \lambda\frac{\dot{V}}{V} + 2\mu\dot{\epsilon}_3. \end{aligned}\right\} \qquad (1)$$

Here λ and μ are the Lame constants; $\dot{\epsilon}_1$, $\dot{\epsilon}_2$, and $\dot{\epsilon}_3$ are the strain rates in the directions given by subscripts; and V is the volume. The dot means a time derivative along the particle path. The time derivative provides an ordered sequence for the incremental stress-strain relationship, but this does not mean that a rate-dependent stress-strain relationship has been introduced. Used in this way, Hooke's law gives natural strain, which means that the strain of the element refers to the current configuration, rather than the original one.

Stress behavior of the material can be thought of as being composed of a stress associated with a uniform hydrostatic pressure (all three normal stresses equal), plus a stress associated with resistance of the material to shear distortion. In describing yielding and plastic flow, we must limit only the stress contributions due to shear distortion. Therefore, each of the stresses σ_1, σ_2, and σ_3 is broken down into a hydrostatic pressure P and a strain deviator S_1, S_2, and S_3:

$$\left.\begin{aligned} \sigma_1 &= -P + S_1, \quad & \dot{\sigma}_1 &= -\dot{P} + \dot{S}_1, \\ \sigma_2 &= -P + S_2, \quad & \dot{\sigma}_2 &= -\dot{P} + \dot{S}_2, \\ \sigma_3 &= -P + S_3, \quad & \dot{\sigma}_3 &= -\dot{P} + \dot{S}_3, \end{aligned}\right\} \qquad (2)$$

where $-P$ is the mean of the three stresses; i.e., $P = -(\sigma_1+\sigma_2+\sigma_3)/3$. The usual notation is followed: stresses are >0 in tension and <0 in compression.

This is just the opposite for pressure, hence the negative sign. The mean normal strain is defined as

$$\theta = \tfrac{1}{3}(\epsilon_1 + \epsilon_2 + \epsilon_3)$$

and

$$\dot{\theta} = \tfrac{1}{3}(\dot{\epsilon}_1 + \dot{\epsilon}_2 + \dot{\epsilon}_3). \tag{3}$$

Similarly, the normal components of the strain deviators are defined as

$$\left.\begin{aligned} \theta_1 &= \epsilon_1 - \theta, \quad & \dot{\theta}_1 &= \dot{\epsilon}_1 - \dot{\theta}, \\ \theta_2 &= \epsilon_2 - \theta, \quad & \dot{\theta}_2 &= \dot{\epsilon}_2 - \dot{\theta}, \\ \theta_3 &= \epsilon_3 - \theta, \quad & \dot{\theta}_3 &= \dot{\epsilon}_3 - \dot{\theta}. \end{aligned}\right\} \tag{4}$$

From the equation of continuity,

$$\dot{\epsilon}_1 + \dot{\epsilon}_2 + \dot{\epsilon}_3 = \frac{\dot{V}}{V}, \tag{5}$$

it follows that

$$\dot{\theta}_1 + \dot{\theta}_2 + \dot{\theta}_3 = 0$$

and

$$\dot{\theta} = \frac{1}{3}\frac{\dot{V}}{V}.$$

With these definitions, Eq. 1 can be written as

$$\left.\begin{aligned} \dot{S}_1 &= 2\mu\left(\dot{\epsilon}_1 - \frac{1}{3}\frac{\dot{V}}{V}\right), \\ \dot{S}_2 &= 2\mu\left(\dot{\epsilon}_2 - \frac{1}{3}\frac{\dot{V}}{V}\right), \\ \dot{S}_3 &= 2\mu\left(\dot{\epsilon}_3 - \frac{1}{3}\frac{\dot{V}}{V}\right), \\ P &= -K\frac{\dot{V}}{V}, \end{aligned}\right\} \tag{6}$$

where

$$K = \lambda + \tfrac{2}{3}\mu = \text{Bulk modulus}.$$

From Eqs. 5 and 6, it follows that

$$\dot{S}_1 + \dot{S}_2 + \dot{S}_3 = 0 \tag{7}$$

and

$$S_1 + S_2 + S_3 = 0, \tag{8}$$

which states that the distortion components of the stress do not contribute to the average pressure.

B. Plastic-flow Region

The yield condition of Von Mises is used to determine the elastic limit.[4] When the principal stresses are known, the yield condition can be written as

$$(\sigma_1 - \sigma_2)^2 + (\sigma_2 - \sigma_3)^2 + (\sigma_3 - \sigma_1)^2 = 2(Y^0)^2, \tag{9}$$

where Y^0 is the yield strength in simple tension.

The left side of Eq. 9 is proportional to the elastic energy of distortion per unit volume or the energy that causes the volume change.[5] Therefore, Eq. 9 states that plastic flow begins when the elastic distortion energy reaches a limiting value $(Y^0)^2/6\mu$ and that this energy remains constant during plastic flow. Thus the term "elastic-plastic" means the state whereby the distortion component of the strained material has been loaded, following Hooke's law, up to a state where the material can no longer store elastic energy. Subsequent distortion will produce plastic flow, and plastic work will be done.

The left side of Eq. 9 also can be interpreted in terms of shear strength. Moreover, there are several ways of viewing Eq. 9, but the point here is that at the elastic limit the left side is equal to a constant. We have chosen to interpret the constant in terms of the yield strength in simple tension, Y^0. If the tension is applied in the σ_1 direction and the lateral stresses σ_2 and σ_3 are zero, then Eq. 9 gives $\sigma_1 = Y^0$. The simple tension term implies two-dimensional flow, since in order for the lateral stresses to be zero there must be strains in the lateral direction; in fact, the ratio $\dot{\epsilon}_2/\dot{\epsilon}_3$ for this case is Poisson's ratio. Also, Eq. 9 implies that the yield strength in tension and compression is the same (absence of Bauschinger effect).

For illustration, in the σ_1, σ_2, σ_3 space of Fig. 1, Eq. 9 describes the surface of a cylinder of radius $\sqrt{2/3}\,Y^0$. The axis of the cylinder is equally inclined to the σ_1, σ_2, σ_3 system of coordinates, as shown in Fig. 1a.

We use the principal stress deviators such that

$$S_1 + S_2 + S_3 = 0 \quad \text{(Eq. 8)}.$$

This is the equation of a plane through the origin of the axis of the principal stresses. Intersection of this plane with the cylinder of Eq. 9 results in a circle (as shown in Fig. 1a). It is assumed that if the stress deviators give a point inside the circle, the material is within the elastic limit.

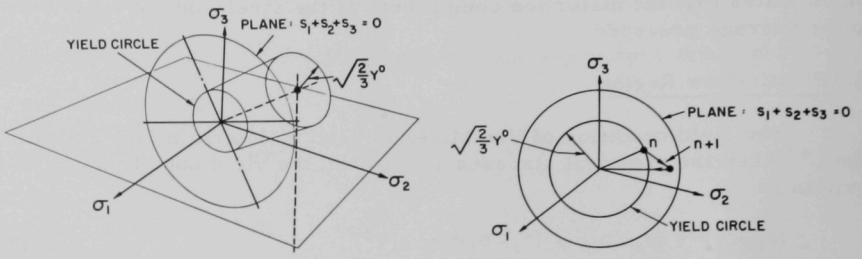

113-1936 (a) (b)

Fig. 1. Von Mises Yield Assumption

When the material is loaded beyond the yield strength and subsequently unloaded, the elastic distortion energy is recovered; work against the material while in the plastic state is not recovered. In other words, the loading and unloading paths are not the same. (In Fig. 2a, the loading path is OAB, the unloading path BC.) It has been shown that the work done on the material during a loading and unloading cycle must be positive or zero, zero only when pure elastic changes occur. Furthermore, the plastic strain increment must be normal to the yield surface that separates the elastic and elastic-plastic states.

We will describe plastic flow by monitoring the stress deviators at the elastic limit. In Fig. 1b, the stresses are shown at state n and, after an incremental strain, at state n + 1. However, state n + 1 is outside the yield surface, and our assumption is that this state cannot be reached. Instead, we will consider that the material flows plastically but the stresses remain at the elastic limit on the yield circle. The plastic component of strain is perpendicular to the yield curve, and it is the stress associated with this component of strain that we wish to limit. Therefore, the new stress state is the point reached by a vector from n and perpendicular to the yield circle. The one-dimensional analogy is shown in Fig. 2a, where the stress $-S_1$ has a maximum value for all strains beyond the elastic limit point A. Thus, to summarize the yield assumption,

$$(S_1 - S_2)^2 + (S_2 - S_3)^2 + (S_3 - S_1)^2 \leq 2(Y^0)^2, \tag{10}$$

$$S_1 + S_2 + S_3 = 0, \tag{11}$$

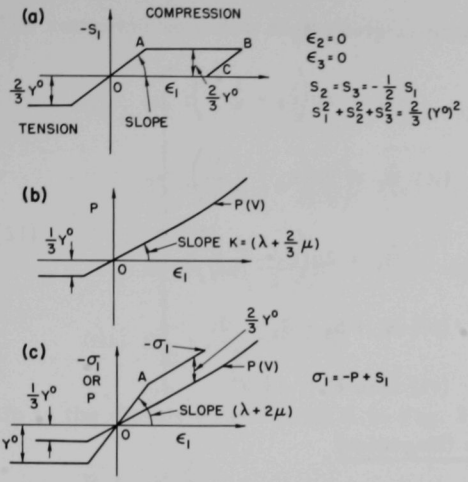

113-1937

Fig. 2. One-dimensional Strain for a Perfectly Plastic Material

which can be written

$$S_1^2 + S_2^2 + S_3^2 \leq \tfrac{2}{3}(Y^0)^2.$$

If an incremental change in the stresses in an element results in a violation of the inequality, each principal stress deviator must be adjusted so that Eq. 11 is again satisfied. Equation 6 is used to calculate the stress deviators. If a point falls outside the yield circle, it is brought back to the circle along the radius vector of the point and hence perpendicular to the yield circle. This is accomplished by multiplying each stress deviator by

$$\sqrt{\tfrac{2}{3}}\,Y^0 \Big/ \sqrt{S_1^2 + S_2^2 + S_3^2}\,.$$

By adjusting the stresses perpendicular to the yield surface, we affect only the plastic components of the stresses. The observed incompressibility of the plastic state is implicit in this procedure. A background pressure state is always present, whether the material is in an elastic or elastic-plastic state, but it is independent of plastic flow. This is in agreement with the observed behavior of ductile metals.

The above formulation applies to a perfectly plastic material, i.e., material that flows plastically without work-hardening (see Fig. 2). For a work-hardening material, the stress ($-S_1$) increases monotonically with strain (ϵ_1) for strains beyond the point A, instead of remaining constant as for the perfectly plastic material shown. Work hardening can be introduced into the calculations by making the constant Y^0 in Eq. 9 a function of the strain energy. Also, when enough work has been done, the value of Y^0 can be set equal to zero. In this way, an all-hydrodynamic description will follow, since the stress deviators will be set equal to zero automatically by the above procedure and the remaining stress will be P. Time-dependent yielding can be represented macroscopically by selecting a high-yield constant Y^0 if the strain rates ($\dot{\epsilon}_1$, $\dot{\epsilon}_2$, and $\dot{\epsilon}_3$) are above some prescribed value.

In the negative pressure region, the pressure is cut off at $P = -\frac{1}{3}Y^0$ consistent with a simple tension test.

The complete equation of state is given by

$$\left.\begin{array}{ll} \sigma_1 = -P + S_1, & \dot{S}_1 = 2\mu\left(\dot{\epsilon}_1 - \frac{1}{3}\frac{\dot{V}}{V}\right), \\ \text{(i)}\quad \sigma_2 = -P + S_2, & \text{(ii)}\quad \dot{S}_2 = 2\mu\left(\dot{\epsilon}_2 - \frac{1}{3}\frac{\dot{V}}{V}\right), \\ \sigma_3 = -P + S_3; & \dot{S}_3 = 2\mu\left(\dot{\epsilon}_3 - \frac{1}{3}\frac{\dot{V}}{V}\right); \\ \text{(iii)}\quad S_1^2 + S_2^2 + S_3^2 \le \frac{2}{3}(Y^0)^2; & \text{(iv)}\quad S_1 + S_2 + S_3 = 0; \\ \text{(v)}\quad P = P(V); & \text{(vi)}\quad \text{Min } P = -\frac{1}{3}Y^0. \end{array}\right\} \tag{12}$$

C. Experimental Equation of State (Hugoniot)

Consider a one-dimensional shock wave traversing a material such that there is a strain in the X direction and zero strain in the Y and Z directions. This is the geometry whereby Hugoniot equation-of-state data are obtained. A shock exists that takes the pressure through an elastic state to an elastic-plastic state.

For one-dimensional flow, the X, Y, Z coordinates are the principal directions, so by Eq. 6 the three stress deviators are

$$\left.\begin{array}{l} \dot{S}_X = 2\mu\left(\dot{\epsilon}_X - \frac{1}{3}\frac{\dot{V}}{V}\right), \\ \dot{S}_Y = 2\mu\left(0 - \frac{1}{3}\frac{\dot{V}}{V}\right), \\ \text{and} \\ \dot{S}_Z = 2\mu\left(0 - \frac{1}{3}\frac{\dot{V}}{V}\right), \end{array}\right\} \tag{13}$$

The total stress in the X direction is

$$\sigma_X = -P + S_X. \tag{14}$$

We will assume that σ_X is obtained by Hugoniot measurements. For one-dimensional flow, the equation of continuity gives

$$\dot{\epsilon}_X = \frac{\dot{V}}{V}.$$

The complete equation of state for one-dimensional geometry is described by

$$\left.\begin{aligned} &\text{(i)}\quad \sigma_X = -P + S_X; \qquad \text{(iv)}\quad S_X + 2S_Y = 0; \\ &\text{(ii)}\quad S_X = 2\mu\left(\frac{\dot{V}}{V} - \frac{1}{3}\frac{\dot{V}}{V}\right), \qquad \text{(v)}\quad P = P(V); \\ &\qquad\quad S_Y = 2\mu\left(-\frac{1}{3}\frac{\dot{V}}{V}\right); \qquad \text{(vi)}\quad \text{Min } P = -\tfrac{1}{3}Y^0. \\ &\text{(iii)}\quad S_X^2 + 2S_Y^2 \le \tfrac{2}{3}(Y^0); \end{aligned}\right\} \tag{15}$$

Up to the elastic limit (point A in Fig. 3),

$$\dot{P} = -K\frac{\dot{V}}{V}$$

and

$$\dot{S}_X = 2\mu\left(\frac{\dot{V}}{V} - \frac{1}{3}\frac{\dot{V}}{V}\right), \tag{16}$$

or

$$P = K \ln V,$$

and

$$S_X = \tfrac{4}{3}\mu \ln V = -2S_Y,$$

$$\sigma_X = K \ln V + \tfrac{4}{3}\mu \ln V = (K + \tfrac{4}{3}\mu) \ln V.$$

At point A,

$$S_X^2 + 2S_Y^2 = \tfrac{2}{3}(Y^0)^2,$$

or

$$\tfrac{24}{9}(\mu \ln A)^2 = \tfrac{2}{3}(Y^0)^2,$$

$$Y^0 = 2\mu|\ln V_A| = \frac{2\mu(\sigma_X)_A}{\lambda + 2\mu}. \tag{17}$$

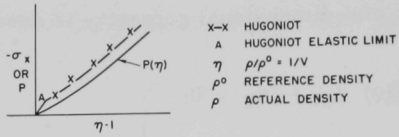

Fig. 3
Hugoniot Curve for a Material-dependent Yield Strength

113-1935

This gives the maximum yield strength Y^0 if the Lame constants and the Hugoniot elastic limit are known.

For points beyond A,

$$S_X^2 + 2S_Y^2 = \tfrac{2}{3}(Y^0)^2,$$

which reduces to

$$S_X = \pm\tfrac{2}{3} Y^0 \text{ (from Eq. 15 iv).} \qquad (18)$$

Therefore, the total stress resulting from a shock from $\sigma_X = 0$ to a point above A is

$$-\sigma_X = P(V) + \tfrac{2}{3} Y^0,$$

where P(V) is the Hugoniot, which is expressed as

$$P(V) = A(n-1) + B(n-1)^2 + C(n-1)^3; \qquad n = \frac{V_0}{V}.$$

Here A, B, and C are constants such that

$$P(V) + \tfrac{2}{3} Y^0$$

reproduces the Hugoniot above point A and

$$p(V) = K \ln V$$

the Hugoniot below the elastic limit A.

Use of an equation of state given in Eq. 15 results in a loading path OAB and an unloading path BCD, as shown in Fig. 4. Experiments on metals in the low-pressure range (0-50 kb) have demonstrated the difference between the P(V) and Hugoniot (σ_X) curves at high pressure (hundreds of kilobars). For some metals, the sound speed behind the shock has been measured to be 20% faster than that predicted by hydrodynamic theory. This gives reason to extend the low-pressure model up to high pressures. From a high pressure, the material unloads first elastically along BC; the slope of the path is characteristic of the elastic unloading velocity. Consequently, the rarefaction wave travels faster than it would if the material unloaded entirely along the P(V) path.

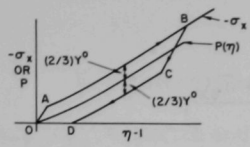

Fig. 4

Stress-Strain Curve for a Perfectly Plastic Material

113-1935

III. BASIC EQUATIONS

This section describes the basic conservation laws, the equation of state, the transformation from Eulerian to Lagrangian coordinates, and the finite-difference formulation of the Lagrangian coordinates.

A. Conservation Laws of Mass, Momentum, and Energy, and the Equation of State

1. Mass

a. Incremental form

$$\rho \, d\forall = \rho^0 \, d\forall^0, \tag{19}$$

where

ρ, $d\forall$ = density and incremental volume change, respectively, at time $t > 0$,

and

ρ^0, $d\forall^0$ = density and undeformed incremental volume, respectively, at time $t = 0$.

b. Differential form

$$\frac{\partial u}{\partial r} + \frac{\partial w}{\partial z} + \frac{u}{r} = \frac{\rho^0}{\rho} = \frac{v^0}{v}, \tag{20}$$

where

u, w = radial and axial velocity, respectively,

and

ρ, v = density and specific volume, respectively.

2. Momentum

$$\rho\ddot{r} = \rho\dot{u} = -\frac{\partial(P - \bar{\sigma}_{rr})}{\partial r} + \frac{\partial \sigma_{rz}}{\partial z} + \frac{2\bar{\sigma}_{rr} + \bar{\sigma}_{zz}}{r}, \tag{21}$$

$$\rho\ddot{z} = \rho\dot{w} = -\frac{\partial(P - \bar{\sigma}_{zz})}{\partial z} + \frac{\partial \sigma_{rz}}{\partial r} + \frac{\sigma_{rz}}{r}, \tag{22}$$

$$P = -\tfrac{1}{3}(\sigma_{rr} + \sigma_{\theta\theta} + \sigma_{zz}), \tag{23}$$

$$\bar{\sigma}_{rr} = \sigma_{rr} + P; \quad \bar{\sigma}_{zz} = \sigma_{zz} + P, \tag{24}$$

and

$$\bar{\sigma}_{\theta\theta} = \sigma_{\theta\theta} + P = -(\bar{\sigma}_{rr} + \bar{\sigma}_{zz}); \quad \bar{\sigma}_{rz} = \sigma_{rz}, \tag{25}$$

where

P = hydrostatic pressure,

$\ddot{u}$, $\dot{w}$ = radial and axial accelerations, respectively,

r, z = radial and axial displacements, respectively,

σ_{rr}, σ_{zz} = radial and axial stresses, respectively,

$\sigma_{\theta\theta}$, σ_{rz} = tangential and shear stresses, respectively,

and

$\bar{\sigma}_{rr}$, $\bar{\sigma}_{zz}$ = radial and axial deviatoric stresses, respectively.

3. Energy

$$\dot{E} = -P\dot{v} + v(\bar{\sigma}_{rr}\dot{\epsilon}_{rr} + \bar{\sigma}_{\theta\theta}\dot{\epsilon}_{\theta\theta} + \bar{\sigma}_{zz}\dot{\epsilon}_{zz} + \sigma_{rz}\dot{\epsilon}_{rz}), \tag{26}$$

$$\dot{\epsilon}_{rr} = \frac{\partial u}{\partial r}; \quad \dot{\epsilon}_{zz} = \frac{\partial w}{\partial z}; \quad \dot{\epsilon}_{rz} = \frac{\partial u}{\partial z} + \frac{\partial w}{\partial r}, \tag{27}$$

and

$$\dot{\epsilon}_{\theta\theta} = \frac{u}{r} = \frac{\dot{v}}{v} - (\dot{\epsilon}_{rr} + \dot{\epsilon}_{zz}), \tag{28}$$

where

E = internal energy per unit mass,

ϵ_{rr}, ϵ_{zz} = radial and axial strains, respectively,

and

$\epsilon_{\theta\theta}$, ϵ_{rz} = tangential and shear strain, respectively.

4. Equation of State

Since no known equation of state prevails for all materials, the form assumed is the Mie-Grüneisen equation of state:

$$P = P_H + \frac{\gamma}{v}(E - E_H), \tag{29}$$

where

$$P_H = A(n-1) + B(n-1)^2 + C(n-1)^3 \quad n = \frac{\rho}{\rho_0} = \frac{v_0}{v}, \tag{30}$$

and

$$E_H = \frac{1}{2} P_H \frac{n-1}{nP_0}, \tag{31}$$

where

P_H = the Hugoniot curve known from experimental data,

γ = Grüneisen's constant,

and

A, B, C = constants.

B. Transformation of Conservation Laws into Lagrangian Coordinates

In the foregoing equations, all dependent variables are functions of the Eulerian coordinates (r, z). For numerical computation, it is desirable to transfer from Eulerian coordinates to Lagrangian coordinates (I, J) for two reasons:

1. In Lagrangian coordinates, the same particle is followed for all time steps; hence conservation of mass is satisfied automatically.

2. In multiregion problems involving contact surfaces, such surfaces can be identified easily, thereby permitting the correct equation of

state to be used. This is not true in Eulerian coordinates. For example, for an arbitrary function $F(r, z)$, the total derivative is

$$dF = \frac{\partial F}{\partial r} dr + \frac{\partial F}{\partial z} dz. \tag{32}$$

If the Eulerian coordinates are written in terms of Lagrangian coordinates,

$$r = r(I, J); \quad z = z(I, J), \tag{33}$$

then

$$\frac{\partial F}{\partial I} = \frac{\partial F}{\partial r}\frac{\partial r}{\partial I} + \frac{\partial F}{\partial z}\frac{\partial z}{\partial I} \tag{34}$$

and

$$\frac{\partial F}{\partial J} = \frac{\partial F}{\partial r}\frac{\partial r}{\partial J} + \frac{\partial F}{\partial z}\frac{\partial z}{\partial J}. \tag{35}$$

Solving Eqs. 34 and 35 for $\frac{\partial F}{\partial r}$ and $\frac{\partial F}{\partial z}$ results in

$$\frac{\partial F}{\partial r} = \frac{\begin{vmatrix} \frac{\partial F}{\partial I} & \frac{\partial z}{\partial I} \\ \frac{\partial F}{\partial J} & \frac{\partial z}{\partial J} \end{vmatrix}}{\begin{vmatrix} \frac{\partial r}{\partial I} & \frac{\partial z}{\partial I} \\ \frac{\partial r}{\partial J} & \frac{\partial z}{\partial J} \end{vmatrix}} = \frac{\frac{\partial(F, z)}{\partial(I, J)}}{\frac{\partial(r, z)}{\partial(I, J)}} \tag{36}$$

and

$$\frac{\partial F}{\partial z} = \frac{\begin{vmatrix} \frac{\partial r}{\partial I} & \frac{\partial F}{\partial I} \\ \frac{\partial r}{\partial J} & \frac{\partial F}{\partial J} \end{vmatrix}}{\begin{vmatrix} \frac{\partial r}{\partial I} & \frac{\partial z}{\partial I} \\ \frac{\partial r}{\partial J} & \frac{\partial z}{\partial J} \end{vmatrix}} = \frac{\frac{\partial(r, F)}{\partial(I, J)}}{\frac{\partial(r, z)}{\partial(I, J)}} = -\frac{\frac{\partial(F, r)}{\partial(I, J)}}{\frac{\partial(r, z)}{\partial(I, J)}}. \tag{37}$$

The denominator turns out to be the area of a zone; hence we define A as

$$A = \frac{\partial(r, z)}{\partial(I, J)}, \tag{38}$$

so that Eqs. 36 and 37 become

$$\left.\begin{aligned} \frac{\partial F}{\partial r} &= \frac{1}{A}\frac{\partial(F, z)}{\partial(I, J)} \\ \text{and} \\ \frac{\partial F}{\partial z} &= -\frac{1}{A}\frac{\partial(F, r)}{\partial(I, J)}. \end{aligned}\right\} \tag{39}$$

Equations 39 represent the general transformation laws from Eulerian to Lagrangian coordinates, and A is the area of the element undergoing transformation.

C. Conservation Laws in Lagrangian Coordinates

1. Mass

For numerical computation, the incremental form Eq. 19 is the best. When the volumes are expressed in terms of Eulerian coordinates, Eq. 19 becomes

$$\frac{\forall}{V} = \frac{\rho^0}{\rho} = \frac{2\pi rA}{2\pi r^0 A^0} = \frac{rA}{r^0 A^0} = \frac{v}{v_0}, \tag{40}$$

where

v^0, ρ^0, r^0, A^0 = variables at time t = 0

and A is given by Eq. 20. Equations 27 and 28 can be used to obtain another differential form of the mass equation. In this case, Eq. 20 becomes

$$\frac{\dot{\rho}}{\rho} = \frac{\dot{V}}{V} = -\left(\dot{\epsilon}_{rr} + \dot{\epsilon}_{\theta\theta} + \dot{\epsilon}_{zz}\right). \tag{41}$$

2. Momentum

On dividing Eqs. 21 and 22 by ρ, we obtain

$$\ddot{r} = \dot{u} = \frac{1}{\rho}\left[-\frac{\partial(P - \bar{\sigma}_{rr})}{\partial r} + \frac{\partial \sigma_{rz}}{\partial z}\right] + \frac{2\bar{\sigma}_{rz} + \bar{\sigma}_{zz}}{\rho r} \tag{42}$$

and

$$\ddot{z} = \dot{w} = \frac{1}{\rho}\left[-\frac{\partial(P - \bar{\sigma}_{zz})}{\partial z} + \frac{\partial \sigma_{rz}}{\partial r}\right] + \frac{\sigma_{rz}}{\rho r}. \tag{43}$$

Using Eq. 40, Eqs. 42 and 43 become

$$\ddot{r} = \dot{u} = \frac{rA}{M^0}\left[-\frac{\partial(P - \bar{\sigma}_{rr})}{\partial r} + \frac{\partial \sigma_{rz}}{\partial z}\right] + \frac{(2\bar{\sigma}_{rr} + \bar{\sigma}_{zz})A}{M^0}, \tag{44}$$

and

$$\ddot{z} = \dot{w} = \frac{rA}{M^0}\left[-\frac{\partial(P - \bar{\sigma}_{zz})}{\partial z} + \frac{\partial \sigma_{rz}}{\partial r}\right] + \frac{\sigma_{rz}A}{M^0} \tag{45}$$

where

$$M^0 = \rho^0 r^0 A^0. \tag{46}$$

The momentum equations are transformed into Lagrangian coordinates using Eq. 39, which gives

$$\ddot{r} = \dot{u} = -\frac{r}{M^0}\left[\frac{\partial(P - \bar{\sigma}_{rr}, z)}{\partial(I, J)} + \frac{\partial(\sigma_{rz}, r)}{\partial(I,J)}\right] + \frac{(2\bar{\sigma}_{rr} + \bar{\sigma}_{zz})A}{M^0}, \tag{47}$$

and

$$\ddot{z} = \dot{w} = \frac{r}{M^0}\left[\frac{\partial(P - \bar{\sigma}_{zz}, r)}{\partial(I, J)} + \frac{\partial(\sigma_{rz}, z)}{\partial(I, J)}\right] + \frac{\sigma_{rz}A}{M^0}. \tag{48}$$

3. Energy

Using Eq. 39, Eqs. 26-28 become

$$\dot{E} = -P\dot{v} + v(\bar{\sigma}_{rr}\dot{\epsilon}_{rr} + \bar{\sigma}_{zz}\dot{\epsilon}_{zz} + \bar{\sigma}_{\theta\theta}\dot{\epsilon}_{\theta\theta} + \sigma_{rz}\epsilon_{rz}), \tag{49}$$

$$\dot{\epsilon}_{rr} = \frac{1}{A}\frac{\partial(u, z)}{\partial(I, J)}; \quad \dot{\epsilon}_{zz} = -\frac{1}{A}\frac{\partial(w, r)}{\partial(I, J)}, \tag{50}$$

$$\dot{\epsilon}_{rz} = \frac{1}{A}\left[\frac{\partial(w, z)}{\partial(I, J)} - \frac{\partial(u, r)}{\partial(I, J)}\right]; \text{ and } \dot{\epsilon}_{\theta\theta} = \frac{\dot{v}}{v} - (\dot{\epsilon}_{rr} + \dot{\epsilon}_{zz}). \tag{51}$$

4. Equation of State

The large P in the energy equation is set equal to the hydrostatic pressure plus an artificial viscosity term, or

$$P = p + q, \tag{52}$$

where

$$q = \begin{cases} (1.2)^2 \rho_0 \frac{A}{v^2} (\dot{v})^2, & \dot{v} < 0; \\ 0, & \dot{v} > 0 \end{cases}. \tag{53}$$

For the pressure p, a Mie-Grüneisen equation of state is used

$$p = p_H + \frac{\gamma}{v} (E - E_H) \tag{54}$$

and

$$p_H = A(n - 1) + B(n - 1)^2 + C(n - 1)^3; \quad n = \frac{\rho}{\rho_0}, \tag{55}$$

where p_H is the Hugoniot equation of state and γ is Grüneisen's constant. E_H is determined from the third Rankine-Hugoniot condition,

$$E_H - E_0 = \tfrac{1}{2}(P_H + P_0)(v_0 - v). \tag{56}$$

Since $E_H >> E_0$ and $P_H >> p_0$, Eq. 56 reduces to

$$E_H = \tfrac{1}{2} P_H \frac{n - 1}{n\rho_0}.$$

For the stresses, Hooke's law holds up to the Hugoniot elastic limit and Von Mises yield criterion holds after that.

a. Hooke's Law

$$\dot{\sigma}_{rr} = 2\mu\left(\dot{\epsilon}_{rr} - \frac{1}{3}\frac{\dot{v}}{v}\right) + \delta_{rr}, \tag{57}$$

$$\dot{\sigma}_{zz} = 2\mu\left(\dot{\epsilon}_{zz} - \frac{1}{3}\frac{\dot{v}}{v}\right) + \delta_{zz}, \tag{58}$$

$$\dot{\sigma}_{\theta\theta} = 2\mu\left(\dot{\epsilon}_{\theta\theta} - \frac{1}{3}\frac{\dot{v}}{v}\right), \tag{59}$$

and

$$\dot{\sigma}_{rz} = \mu \dot{\epsilon}_{rz} + \delta_{rz}, \tag{60}$$

where

μ = shear modulus,

δ = correction for rotation during time step in computation,

$$\delta_{rr} = -\delta_{zz}, \tag{61}$$

$$\delta_{zz} = \frac{\bar{\sigma}_{zz} - \bar{\sigma}_{rr}}{2} (\cos 2\omega - 1) + \sigma_{rz} \sin 2\omega, \tag{62}$$

$$\delta_{rz} = \sigma_{rz} (\cos 2\omega - 1) - \frac{\bar{\sigma}_{zz} - \bar{\sigma}_{rr}}{2} \sin 2\omega, \tag{63}$$

and

$$\sin \omega = \frac{\Delta t^{m+\frac{1}{2}}}{2} \left(\frac{\partial u}{\partial z} - \frac{\partial w}{\partial r} \right). \tag{64}$$

Using Eq. 39, Eq. 64 becomes

$$\sin \omega = - \frac{\Delta t^{m+\frac{1}{2}}}{2A} \left[\frac{\partial (u, r)}{\partial (I, J)} + \frac{\partial (w, z)}{\partial (I, J)} \right]. \tag{65}$$

b. Principal Stresses

$$S_1 = \frac{\bar{\sigma}_{rr} + \bar{\sigma}_{zz}}{2} + \tfrac{1}{2} \left[(\bar{\sigma}_{zz} - \bar{\sigma}_{rr})^2 + (2\sigma_{rz})^2 \right]^{\frac{1}{2}}, \tag{66}$$

$$S_2 = \frac{\bar{\sigma}_{rr} + \bar{\sigma}_{zz}}{2} - \tfrac{1}{2} \left[(\bar{\sigma}_{zz} - \bar{\sigma}_{rr})^2 + (2\sigma_{rz})^2 \right]^{\frac{1}{2}}, \tag{67}$$

and

$$S_3 = \bar{\sigma}_{\theta\theta}, \tag{68}$$

where

$\bar{\sigma}_{\theta\theta}$ is a principal stress.

c. Von Mises Yield Condition

$$2J = S_1^2 + S_2^2 + S_3^2 = \bar{\sigma}_{rz}^2 + \bar{\sigma}_{zz}^2 + \bar{\sigma}_{\theta\theta}^2 + 2\sigma_{rz}^2 \leq \tfrac{2}{3}(Y^0)^2, \tag{69}$$

where Y^0 is the yield strength of the material.

In tension, the hydrostatic pressure can take a minimum of

$$p = -\tfrac{1}{3} Y^0. \tag{70}$$

D. Finite-difference Equations in Lagrangian Coordinates

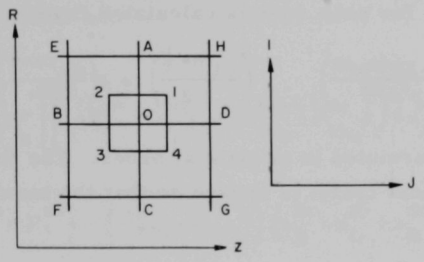

Zone Identification for Finite-difference Equations

The correspondence between the letters and numbers in the illustration, with Lagrangian coordinates is

$1 = I + \frac{1}{2},\ J + \frac{1}{2}$	$0 = I,\ J$	$E = I + 1,\ J - 1$
$2 = I + \frac{1}{2},\ J - \frac{1}{2}$	$A = I + 1,\ J$	$F = I - 1,\ J - 1$
$3 = I - \frac{1}{2},\ J - \frac{1}{2}$	$B = I,\ J - 1$	$G = I - 1,\ J + 1$
$4 = I - \frac{1}{2},\ J + \frac{1}{2}$	$C = I - 1,\ J$	$H = I + 1,\ J + 1.$
	$D = I,\ J + 1$	

For converting the differential equations in Lagrangian coordinates into finite-difference form, the following equations are needed:

$$\frac{\partial(F, r)}{\partial(I, J)} = \tfrac{1}{8}[(F_2 - F_4)(r_A - r_C + r_D - r_B) - (F_1 - F_3)(r_A - r_C + r_B - r_D)]; \tag{71}$$

$$\frac{\partial(F, z)}{\partial(I, J)} = \tfrac{1}{8}[(F_2 - F_4)(z_A - z_C + z_D - z_B) - (F_1 - F_3)(z_A - z_C + z_B - z_D)]. \tag{72}$$

In the equations that follow, the subscripts refer to the zone identification, and the superscripts to the time of occurrence.

At a given time t^m, all the quantities $\dot{u}^{m-1}$, $\dot{w}^{m-1}$, $u^{m-\frac{1}{2}}$, $w^{m-\frac{1}{2}}$, r^m, and z^m at point 0, and E^m, A^m, p^m, q^m, p^m, v^m, σ^m_{rr}, $\sigma^m_{\theta\theta}$, σ^m_{zz}, σ^m_{rz}, $\bar{\sigma}^m_{rr}$, $\bar{\sigma}^m_{\theta\theta}$, $\bar{\sigma}^m_{zz}$, S_1^m, S_2^m, S_3^m, $\dot{\epsilon}^m_{rr}$, $\dot{\epsilon}^m_{zz}$, $\dot{\epsilon}^m_{rz}$, $\dot{v}^{m-\frac{1}{2}}$, and $\dot{A}^m$ at points 1, 2, 3, and 4 are known from the initial data for $m = 0$ and from the computation of the previous cycle for $m > 1$.

At the beginning of a new cycle, t^{m+1} is computed from

$$t^{m+1} = t^m + \Delta t^{m+\frac{1}{2}}, \tag{73}$$

where $\Delta t^{m+\frac{1}{2}}$ is the time step determined from stability considerations. The White stability number for each zone is calculated from

$$\left|\left(\frac{w}{1.2}\right)^2\right|^m_{1,2,3,4} = \left(\frac{1+3p^m v^m}{p^0 A^m}\right)_{1,2,3,4}\left(\frac{\Delta t^{m-\frac{1}{2}}}{1.2}\right)^2 + 4\left(\frac{\Delta v^{m-\frac{1}{2}}}{v^m}\right)_{1,2,3,4}, \tag{74}$$

where the subscripts are permuted in sequential order. The time interval $\Delta t^{m+\frac{1}{2}}$, to be used for the next cycle, is chosen so that the maximum of the stability numbers with

$$\Delta t^{m+\frac{1}{2}} \rightarrow \Delta t^{m-\frac{1}{2}} \tag{75}$$

satisfies

$$0.035 \leq \left(\frac{w}{1.2}\right)^2 \leq 0.14, \tag{76}$$

or

$$0.225 < w_{max} < 0.45. \tag{77}$$

Once $\Delta t^{m+\frac{1}{2}}$ is found, the Δt^m is determined from

$$\Delta t^m = \frac{\Delta t^{m+\frac{1}{2}} + \Delta t^{m-\frac{1}{2}}}{2}. \tag{78}$$

Next, the accelerations $\dot{u}^m$ and $\dot{w}^m$ are calculated. For this purpose, Eqs. 47 and 48 are used. From Eq. 46,

$$(M^0)_0 = (\rho^0 r^0 A^0)_0. \tag{79}$$

Equation 79 is approximated by assuming that

$$(M^0)_0 = \tfrac{1}{4}(M_1^0 + M_2^0 + M_3^0 + M_4^0), \tag{80}$$

$$M^0_{1,2,3,4} = \rho^0_{1,2,3,4}\, r^0_{1,2,3,4}\, A^0_{1,2,3,4}, \tag{81}$$

$$r^0_{1,2,3,4} = \frac{1}{4}\left(r^0_{0,0,0,0} + r^0_{D,A,B,C} + r^0_{H,E,F,G} + r^0_{A,B,C,D}\right), \tag{82}$$

and

$$A^0_{1,2,3,4} = \frac{1}{2}\left[\left(r^0_{A,E,B,D} - r^0_{D,0,C,G}\right)\left(z^0_{H,A,0,D} - z^0_{0,B,F,C}\right) - \left(r^m_{H,A,0,D} - r^0_{0,B,F,C}\right)\left(z^0_{A,E,B,D} - z^0_{D,0,C,G}\right)\right]. \tag{83}$$

The accelerations are

$$\dot{u}^m_0 = -\frac{r^m_0}{8(M^0)_0}\left[\left\{\left(\left(P^m_2 - P^m_4\right) - \left(\bar{\sigma}^m_{rr_2} - \bar{\sigma}^m_{rr_4}\right)\right)\left(z^m_A - z^m_C + z^m_D - z^m_B\right) - \left(\left(P^m_1 - P^m_3\right) - \left(\bar{\sigma}^m_{rr_1} - \bar{\sigma}_{rr_3}\right)\right)\left(z^m_A - z^m_C + z^m_B - z^m_D\right)\right\} + \left\{\left(\sigma^m_{rz_2} - \sigma^m_{rz_4}\right)\left(r^m_A - r^m_C + r^m_D - r^m_B\right) - \left(\sigma^m_{rz_1} - \sigma^m_{rz_3}\right)\left(r^m_A - r^m_C + r^m_B - r^m_D\right)\right\}\right] + \left(\frac{\left(2\bar{\sigma}^m_{rr} + \bar{\sigma}^m_{zz}\right)A^m}{M^0}\right)_0, \tag{84}$$

$$w^m_0 = \frac{r^m_0}{8(M^0)_0}\left[\left\{\left(\left(P^m_2 - P^m_4\right) - \left(\bar{\sigma}^m_{zz_2} - \bar{\sigma}^m_{zz_4}\right)\right)\left(r^m_A - r^m_C + r^m_D - r^m_B\right) - \left(\left(P^m_1 - P^m_3\right) - \left(\bar{\sigma}^m_{zz_1} - \bar{\sigma}^m_{zz_3}\right)\right)\left(r^m_A - r^m_C + r^m_B - r^m_D\right)\right\} + \left\{\left(\sigma^m_{rz_2} - \sigma^m_{rz_4}\right)\left(z^m_A - z^m_C + z^m_D - z^m_B\right) - \left(\sigma^m_{rz_1} - \sigma^m_{rz_3}\right)\left(z^m_A - z^m_C + z^m_B - z^m_D\right)\right\}\right] + \left(\frac{\sigma^m_{rz} A^m}{M^0}\right)_0, \tag{85}$$

$$\left(\frac{\left(2\bar{\sigma}^{m}_{rr}+\bar{\sigma}^{m}_{zz}\right)A^{m}}{M^{0}}\right)_{0} = \frac{1}{4}\left\{\left(\frac{\left(2\bar{\sigma}^{m}_{rr}+\bar{\sigma}^{m}_{zz}\right)A^{m}}{M^{0}}\right)_{1} + \left(\frac{\left(2\bar{\sigma}^{m}_{rr}+\bar{\sigma}^{m}_{zz}\right)A^{m}}{M^{0}}\right)_{2} + \left(\frac{\left(2\bar{\sigma}^{m}_{rr}+\bar{\sigma}^{m}_{zz}\right)A^{m}}{M^{0}}\right)_{3} + \left(\frac{\left(2\bar{\sigma}^{m}_{rr}+\bar{\sigma}^{m}_{zz}\right)A^{m}}{M^{0}}\right)_{4}\right\}, \tag{86}$$

$$\left(\frac{\sigma^{m}_{rz}A^{m}}{M^{0}}\right)_{0} = \frac{1}{4}\left[\left(\frac{\sigma^{m}_{rz}A^{m}}{M^{0}}\right)_{1} + \left(\frac{\sigma^{m}_{rz}A^{m}}{M^{0}}\right)_{2} + \left(\frac{\sigma^{m}_{rz}A^{m}}{M^{0}}\right)_{3} + \left(\frac{\sigma^{m}_{rz}A^{m}}{M^{0}}\right)_{4}\right], \tag{87}$$

and

$$A^{m}_{1,2,3,4} = \frac{1}{2}\left[\left(r^{m}_{A,E,B,D} - r^{m}_{D,0,C,G}\right)\left(z^{m}_{H,A,0,D} - z^{m}_{0,B,F,C}\right) - \left(r^{m}_{H,A,0,D} - r^{m}_{0,B,F,C}\right)\left(z^{m}_{A,E,B,D} - z^{m}_{D,0,C,G}\right)\right]. \tag{88}$$

In Eqs. 84 and 85, there is the following complication: If r^{m}_{0} is taken for r = 0, then $\dot{u}$ and $\dot{z}$ are zero, which is physically incorrect. Thus the term $r^{m}_{0}/(M^{0})_{0}$ in both equations must be modified in the following manner. Since the mass of each volume is constant with time in Lagrangian coordinates,

$$M^{0} = \rho^{0}r^{0}A^{0} = \rho^{m}r^{m}A^{m} \tag{89}$$

and

$$\frac{r^{m}}{M^{0}} = \frac{r^{m}}{\rho^{m}r^{m}A^{m}} = \frac{1}{\rho^{m}A^{m}}. \tag{90}$$

Thus,

$$\frac{r^{m}_{0}}{(M^{0})_{0}} = \frac{1}{(\rho^{m}A^{m})_{0}}, \tag{91}$$

$$(\rho^{m}A^{m})_{0} = \frac{1}{4}\left[(\rho^{m}A^{m})_{1} + (\rho^{m}A^{m})_{2} + (\rho^{m}A^{m})_{3} + (\rho^{m}A^{m})_{4}\right], \tag{92}$$

and

$$\rho^{m}_{1,2,3,4} = \frac{M^{0}_{1,2,3,4}}{r^{m}_{1,2,3,4} A^{m}_{1,2,3,4}} . \tag{93}$$

Therefore, the final form for the accelerations is

$$\begin{aligned}
\dot{u}^{m}_{0} = \frac{-1}{8(\rho^{m} A^{m})_{0}} \Bigg(& \Bigg\{ \left[\left(p^{m}_{2} - p^{m}_{4} \right) - \left(\bar{\sigma}^{m}_{rr_2} - \bar{\sigma}^{m}_{rr_4} \right) \right] \left(z^{m}_{A} - z^{m}_{C} + z^{m}_{D} - z^{m}_{B} \right) \\
& - \left[\left(P^{m}_{1} - P^{m}_{3} \right) - \left(\bar{\sigma}^{m}_{rr_1} - \bar{\sigma}^{m}_{rr_3} \right) \right] \left(z^{m}_{A} - z^{m}_{C} + z^{m}_{B} - z^{m}_{D} \right) \Bigg\} \\
& + \Bigg\{ \left[\left(\sigma^{m}_{rz_2} - \sigma^{m}_{rz_4} \right) \left(r^{m}_{A} - r^{m}_{C} + r^{m}_{D} - r^{m}_{B} \right) \right. \\
& \left. - \left(\sigma^{m}_{rz_1} - \sigma^{m}_{rz_3} \right) \left(r^{m}_{A} - r^{m}_{C} + r^{m}_{B} - r^{m}_{D} \right) \right] \Bigg\} \Bigg) \\
& + \left(\frac{\left(2\bar{\sigma}^{m}_{rr} + \bar{\sigma}^{m}_{zz} \right) A^{m}}{M^{0}} \right)_{0}
\end{aligned} \tag{94}$$

and

$$\begin{aligned}
\dot{w}^{m}_{0} = \frac{1}{8(\rho^{m} A^{m})_{0}} \Bigg(& \Bigg\{ \left[\left(P^{m}_{2} - P^{m}_{4} \right) - \left(\bar{\sigma}^{m}_{zz_2} - \bar{\sigma}^{m}_{zz_4} \right) \right] \left(r^{m}_{A} - r^{m}_{C} + r^{m}_{D} r^{m}_{B} \right) \\
& - \left[\left(P^{m}_{1} - P^{m}_{3} \right) - \left(\bar{\sigma}^{m}_{zz_1} - \bar{\sigma}^{m}_{zz_3} \right) \right] \left(r^{m}_{A} - r^{m}_{C} + r^{m}_{B} - r^{m}_{D} \right) \Bigg\} \\
& + \Bigg\{ \left[\left(\sigma^{m}_{rz_2} - \sigma^{m}_{rz_4} \right) \left(z^{m}_{A} - z^{m}_{C} + z^{m}_{D} - z^{m}_{B} \right) \right. \\
& \left. - \left(\sigma^{m}_{rz_1} - \sigma^{m}_{rz_3} \right) \left(z^{m}_{A} - z^{m}_{C} + z^{m}_{B} - z^{m}_{D} \right) \right] \Bigg\} \Bigg) \\
& + \left(\frac{\sigma^{m}_{rz} A^{m}}{M^{0}} \right)_{0} .
\end{aligned} \tag{95}$$

The other equations remain the same. New velocities are calculated from

$$u_0^{m+\frac{1}{2}} = u_0^{m-\frac{1}{2}} + \Delta t^m \cdot {}^m u_0 \tag{96}$$

and

$$w_0^{m+\frac{1}{2}} = w_0^{m-\frac{1}{2}} + \Delta t^m \cdot {}^m w_0, \tag{97}$$

where Δt^m is given by Eq. 78.

Next, the new positions are calculated from

$$r_0^{m+1} = r_0^m + \Delta t^{m+\frac{1}{2}} u_0^{m+\frac{1}{2}} \tag{98}$$

and

$$z_0^{m+1} = z_0^m + \Delta t^{m+\frac{1}{2}} w_0^{m+\frac{1}{2}}, \tag{99}$$

and the new areas from

$$A_{1,2,3,4}^{m+1} = \frac{1}{2}\left[\left(r_{A,E,B,D}^{m+1} - r_{D,0,C,G}^{m+1}\right)\left(z_{H,A,0,D}^{m+1} - z_{0,B,F,C}^{m+1}\right)\right.$$

$$\left. - \left(r_{H,A,0,D}^{m+1} - r_{0,B,F,C}^{m+1}\right)\left(z_{A,E,B,D}^{m+1} - z_{D,0,C,G}^{m+1}\right)\right] \tag{100}$$

In the rest of the equations, a number of quantities will be needed at $t^{m+\frac{1}{2}}$. These are obtained by substituting

$$F^{m+\frac{1}{2}} = \frac{F^{m+1} + F^m}{2} \tag{101}$$

for

$$F = r, z, A, v, \bar{\sigma}_{rr}, \bar{\sigma}_{\theta\theta}, \bar{\sigma}_{zz}, \sigma_{rz}. \tag{102}$$

Specific volume and specific volume rate are calculated from

$$v_{1,2,3,4}^m = \frac{r_{1,2,3,4}^m A_{1,2,3,4}^m}{(M^0)_{1,2,3,4}}, \quad v_{1,2,3,4}^{m+1} = \frac{r_{1,2,3,4}^{m+1} A_{1,2,3,4}^{m+1}}{(M^0)_{1,2,3,4}}; \tag{103}$$

and

$$\dot{v}^{m+\frac{1}{2}}_{1,2,3,4} = \frac{v^{m+1}_{1,2,3,4} - v^{m}_{1,2,3,4}}{\Delta t^{m+\frac{1}{2}}}, \quad v^{m+\frac{1}{2}}_{1,2,3,4} = \frac{v^{m+1}_{1,2,3,4} + v^{m}_{1,2,3,4}}{2}. \tag{104}$$

Strain rates are calculated from Eqs. 50 and 51 to give

$$(\dot{\epsilon}_{rr})^{m+\frac{1}{2}}_{1,2,3,4} = \frac{1}{2A^{m+\frac{1}{2}}_{1,2,3,4}} \left[\left(u^{m+\frac{1}{2}}_{A,E,B,D} - u^{m+\frac{1}{2}}_{D,0,C,G} \right) \left(z^{m+\frac{1}{2}}_{H,A,0,D} - z^{m+\frac{1}{2}}_{0,B,F,C} \right) \right.$$

$$\left. - \left(u^{m+\frac{1}{2}}_{H,A,0,D} - u^{m+\frac{1}{2}}_{0,B,F,C} \right) \left(z^{m+\frac{1}{2}}_{A,E,B,D} - z^{m+\frac{1}{2}}_{D,0,C,G} \right) \right], \tag{105}$$

$$(\dot{\epsilon}_{zz})^{m+\frac{1}{2}}_{1,2,3,4} = \frac{1}{2A^{m+\frac{1}{2}}_{1,2,3,4}} \left[\left(w^{m+\frac{1}{2}}_{A,E,B,D} - w^{m+\frac{1}{2}}_{D,0,C,G} \right) \left(r^{m+\frac{1}{2}}_{H,A,0,D} - r^{m+\frac{1}{2}}_{0,B,F,C} \right) \right.$$

$$\left. - \left(w^{m+\frac{1}{2}}_{H,A,0,D} - w^{m+\frac{1}{2}}_{0,B,F,C} \right) \left(r^{m+\frac{1}{2}}_{A,F,B,D} - r^{m+\frac{1}{2}}_{D,0,C,G} \right) \right], \tag{106}$$

$$(\dot{\epsilon}_{\theta\theta})^{m+\frac{1}{2}}_{1,2,3,4} = \left(\frac{\dot{v}}{v} \right)^{m+\frac{1}{2}}_{1,2,3,4} - \left[(\dot{\epsilon}_{rr})^{m+\frac{1}{2}}_{1,2,3,4} + (\dot{\epsilon}_{zz})^{m+\frac{1}{2}}_{1,2,3,4} \right], \tag{107}$$

and

$$(\dot{\epsilon}_{rz})^{m+\frac{1}{2}}_{1,2,3,4} = \frac{1}{2A^{m+\frac{1}{2}}_{1,2,3,4}} \left\{ \left[\left(w^{m+\frac{1}{2}}_{A,E,B,0} - w^{m+\frac{1}{2}}_{D,0,C,G} \right) \left(z^{m+\frac{1}{2}}_{H,A,0,D} - z^{m+\frac{1}{2}}_{0,B,F,C} \right) \right. \right.$$

$$\left. - \left(w^{m+\frac{1}{2}}_{H,A,0,D} - w^{m+\frac{1}{2}}_{0,B,F,C} \right) \left(z^{m+\frac{1}{2}}_{A,E,B,D} - z^{m+\frac{1}{2}}_{D,0,C,G} \right) \right]$$

$$- \left[\left(u^{m+\frac{1}{2}}_{A,E,B,D} - u^{m+\frac{1}{2}}_{0,B,F,C} \right) \left(r^{m+\frac{1}{2}}_{H,A,0,D} - r^{m+\frac{1}{2}}_{0,B,F,C} \right) \right.$$

$$\left. \left. - \left(u^{m+\frac{1}{2}}_{H,A,0,D} - u^{m+\frac{1}{2}}_{0,B,F,C} \right) \left(r^{m+\frac{1}{2}}_{A,E,B,D} - r^{m+\frac{1}{2}}_{D,0,C,G} \right) \right] \right\}. \tag{108}$$

Total strains are calculated by multiplying Eqs. 105-108 by $\Delta t^{m+\frac{1}{2}}$, giving

$$(\Delta\epsilon_{rr})^{m+\frac{1}{2}}_{1,2,3,4} = (\dot{\epsilon}_{rr})^{m+\frac{1}{2}}_{1,2,3,4}\,\Delta t^{m+\frac{1}{2}}, \tag{109}$$

$$(\Delta\epsilon_{zz})^{m+\frac{1}{2}}_{1,2,3,4} = (\dot{\epsilon}_{zz})^{m+\frac{1}{2}}_{1,2,3,4}\,\Delta t^{m+\frac{1}{2}}, \tag{110}$$

$$(\Delta\epsilon_{rz})^{m+\frac{1}{2}}_{1,2,3,4} = (\dot{\epsilon}_{rz})^{m+\frac{1}{2}}_{1,2,3,4}\,\Delta t^{m+\frac{1}{2}}, \tag{111}$$

and

$$(\Delta\epsilon_{\theta\theta})^{m+\frac{1}{2}}_{1,2,3,4} = (\dot{\epsilon}_{\theta\theta})^{m+\frac{1}{2}}_{1,2,3,4}\,\Delta t^{m+\frac{1}{2}}. \tag{112}$$

The elastic deviator stresses are calculated next:

$$\left(\frac{\Delta v}{v}\right)^{m+\frac{1}{2}}_{1,2,3,4} = \left(\frac{\dot{v}}{v}\right)^{m+\frac{1}{2}}_{1,2,3,4}\Delta t^{m+\frac{1}{2}} = \frac{v^{m+1}_{1,2,3,4} - v^{m}_{1,2,3,4}}{v^{m+\frac{1}{2}}_{1,2,3,4}} \tag{113}$$

$$(\bar{\sigma}_{rr})^{m+1}_{1,2,3,4} = (\bar{\sigma}_{rr})^{m}_{1,2,3,4} + \Delta t^{m+\frac{1}{2}}\left(\dot{\bar{\sigma}}_{rr}\right)^{m+\frac{1}{2}}_{1,2,3,4}$$

$$= (\bar{\sigma}_{rr})^{m}_{1,2,3,4} + 2\mu\left[(\Delta\epsilon_{rr})^{m+\frac{1}{2}}_{1,2,3,4} - \frac{1}{3}\left(\frac{\Delta v}{v}\right)^{m+\frac{1}{2}}_{1,2,3,4}\right] + \delta_{rr}, \tag{114}$$

$$(\bar{\sigma}_{zz})^{m+1}_{1,2,3,4} = (\bar{\sigma}_{zz})^{m}_{1,2,3,4} + \Delta t^{m+\frac{1}{2}}\left(\dot{\bar{\sigma}}_{zz}\right)^{m+\frac{1}{2}}_{1,2,3,4}$$

$$= (\bar{\sigma}_{zz})^{m}_{1,2,3,4} + 2\mu\left[(\Delta\epsilon_{zz})^{m+\frac{1}{2}}_{1,2,3,4} - \frac{1}{3}\left(\frac{\Delta v}{v}\right)^{m+\frac{1}{2}}_{1,2,3,4}\right] + \delta_{zz}, \tag{115}$$

$$(\bar{\sigma}_{\theta\theta})^{m+1}_{1,2,3,4} = (\bar{\sigma}_{\theta\theta})^{m}_{1,2,3,4} + \Delta t^{m+\frac{1}{2}}\left(\dot{\bar{\sigma}}_{\theta\theta}\right)^{m+\frac{1}{2}}_{1,2,3,4}$$

$$= (\bar{\sigma}_{\theta\theta})^{m}_{1,2,3,4} + 2\mu\left[(\Delta\epsilon_{\theta\theta})^{m+\frac{1}{2}}_{1,2,3,4} - \frac{1}{3}\left(\frac{\Delta v}{v}\right)^{m+\frac{1}{2}}_{1,2,3,4}\right], \tag{116}$$

$$(\sigma_{rz})^{m+1}_{1,2,3,4} = (\sigma_{rz})^{m}_{1,2,3,4} + \Delta t^{m+\frac{1}{2}} (\dot{\sigma}_{rz})^{m+\frac{1}{2}}_{1,2,3,4}$$

$$= (\sigma_{rz})^{m}_{1,2,3,4} + 2\mu \left[(\Delta \epsilon_{rz})^{m+\frac{1}{2}}_{1,2,3,4} - \frac{1}{3} \left(\frac{\Delta v}{v} \right)^{m+\frac{1}{2}}_{1,2,3,4} \right] + \delta_{rz}, \tag{117}$$

$$(\delta_{rr})^{m}_{1,2,3,4} = -(\delta_{zz})^{m}_{1,2,3,4}, \tag{118}$$

$$(\delta_{zz})^{m}_{1,2,3,4} = \left[\frac{(\bar{\sigma}_{zz})^{m}_{1,2,3,4} - (\bar{\sigma}_{rr})^{m}_{1,2,3,4}}{2} \right] \left[(\cos 2\omega)^{m+\frac{1}{2}}_{1,2,3,4} - 1 \right]$$

$$+ (\sigma_{rz})^{m}_{1,2,3,4} (\sin 2\omega)^{m+\frac{1}{2}}_{1,2,3,4}, \tag{119}$$

$$(\delta_{rz})^{m}_{1,2,3,4} = (\sigma_{rz})^{m}_{1,2,3,4} \left[(\cos 2\omega)^{m+\frac{1}{2}}_{1,2,3,4} - 1 \right]$$

$$- \left[\frac{(\bar{\sigma}_{zz})^{m}_{1,2,3,4} - (\bar{\sigma}_{rr})^{m}_{1,2,3,4}}{2} \right] (\sin 2\omega)^{m+\frac{1}{2}}_{1,2,3,4}, \tag{120}$$

$$(\sin \omega)^{m+\frac{1}{2}}_{1,2,3,4} = - \frac{\Delta t^{m+\frac{1}{2}}}{4A^{m+\frac{1}{2}}_{1,2,3,4}} \left\{ \left[\left(u^{m+\frac{1}{2}}_{A,E,B,D} - u^{m+\frac{1}{2}}_{D,0,C,G} \right) \left(r^{m+\frac{1}{2}}_{H,A,0,D} - r^{m+\frac{1}{2}}_{0,B,F,C} \right) \right.\right.$$

$$\left. - \left(u^{m+\frac{1}{2}}_{H,A,0,D} - u^{m+\frac{1}{2}}_{0,B,F,C} \right) \left(r^{m+\frac{1}{2}}_{A,E,B,D} - r^{m+\frac{1}{2}}_{D,0,C,G} \right) \right]$$

$$- \left[\left(w^{m+\frac{1}{2}}_{A,E,B,D} - w^{m+\frac{1}{2}}_{D,0,C,G} \right) \left(z^{m+\frac{1}{2}}_{H,A,0,D} - z^{m+\frac{1}{2}}_{0,B,F,C} \right) \right.$$

$$\left.\left. - \left(w^{m+\frac{1}{2}}_{H,A,0,D} - w^{m+\frac{1}{2}}_{0,B,F,C} \right) \left(z^{m+\frac{1}{2}}_{A,E,B,D} - z^{m+\frac{1}{2}}_{D,0,C,G} \right) \right] \right\}. \tag{121}$$

The principal stresses are given by

$$(S_1)^{m+1}_{1,2,3,4} = \frac{(\bar{\sigma}_{rr})^{m+1}_{1,2,3,4} + (\bar{\sigma}_{zz})^{m+1}_{1,2,3,4}}{2}$$

$$+ \frac{1}{2}\left\{\left[(\bar{\sigma}_{zz})^{m+1}_{1,2,3,4} - (\bar{\sigma}_{rr})^{m+1}_{1,2,3,4}\right]^2 + \left[(2\sigma_{rz})^{m+1}_{1,2,3,4}\right]^2\right\}^{\frac{1}{2}}, \tag{122}$$

$$(S_2)^{m+1}_{1,2,3,4} = \frac{(\bar{\sigma}_{rr})^{m+1}_{1,2,3,4} + (\bar{\sigma}_{zz})^{m+1}_{1,2,3,4}}{2}$$

$$- \frac{1}{2}\left\{\left[(\bar{\sigma}_{zz})^{m+1}_{1,2,3,4} - (\bar{\sigma}_{rr})^{m+1}_{1,2,3,4}\right]^2 + \left[(2\sigma_{rz})^{m+1}_{1,2,3,4}\right]^2\right\}^{\frac{1}{2}}, \tag{123}$$

and

$$(S_3)^{m+1}_{1,2,3,4} = (\bar{\sigma}_{\theta\theta})^{m+1}_{1,2,3,4}. \tag{124}$$

The Von Mises Yield Condition is given by

$$2J^{m+1}_{1,2,3,4} = \left[(S_1)^{m+1}_{1,2,3,4}\right]^2 + \left[(S_2)^{m+1}_{1,2,3,4}\right]^2 + \left[(S_3)^{m+1}_{1,2,3,4}\right]^2; \tag{125}$$

then,

$$K^{m+1}_{1,2,3,4} = 2J^{m+1}_{1,2,3,4} - \tfrac{2}{3}(Y^0)^2. \tag{126}$$

If $K^{m+1} < 0$, the deviator stresses are used unchanged in calculation. If $K^{m+1} > 0$, the terms $\bar{\sigma}^{m+1}_{rr}$, $\bar{\sigma}^{m+1}_{zz}$, $\bar{\sigma}^{m+1}_{\theta\theta}$, and σ^{m+1}_{rz} are multiplied by

$$\frac{\sqrt{\frac{2}{3}}Y^0}{\sqrt{2J^{m+1}}}, \tag{127}$$

and the new values are used.

The next quantities--pressure and internal energy--are determined by solving the equation of state and the energy equation simultaneously from

$$P^{m+1}_{1,2,3,4} = P^{m+1}_{1,2,3,4} + q^{m+1}_{1,2,3,4}, \tag{128}$$

$$P^{m+1}_{1,2,3,4} = P_H + \frac{\gamma}{v^{m+1}_{1,2,3,4}} \left(E^{m+1}_{1,2,3,4} - E_H \right), \tag{129}$$

$$q^{m+1}_{1,2,3,4} = \begin{cases} \dfrac{(1.2)^2 \, \rho^0_{1,2,3,4} A^{m+1}_{1,2,3,4}}{\left(v^{m+1}_{1,2,3,4} \right)^2} \left(\dot{v}^{m+\frac{1}{2}}_{1,2,3,4} \right)^2 & \Delta v < 0 \\ 0 & \Delta v > 0 \end{cases}, \tag{130}$$

and

$$E^{m+1}_{1,2,3,4} = E^{m}_{1,2,3,4} - \frac{P^{m+1}_{1,2,3,4} + P^{m}_{1,2,3,4}}{2} \left(v^{m+1}_{1,2,3,4} - v^{m}_{1,2,3,4} \right)$$

$$+ v^{m+\frac{1}{2}}_{1,2,3,4} \left(\bar{\sigma}_{rr} \Delta \epsilon_{rr} + \bar{\sigma}_{zz} \Delta \epsilon_{zz} + \bar{\sigma}_{\theta\theta} \Delta \epsilon_{\theta\theta} + \sigma_{rz} \Delta \epsilon_{rz} \right)^{m+\frac{1}{2}}_{1,2,3,4}. \tag{131}$$

The total stresses computed from

$$\left.\begin{aligned} (\sigma_{rr})^{m+1}_{1,2,3,4} &= (\bar{\sigma}_{rr})^{m+1}_{1,2,3,4} - P^{m+1}_{1,2,3,4}; \\ (\sigma_{zz})^{m+1}_{1,2,3,4} &= (\bar{\sigma}_{zz})^{m+1}_{1,2,3,4} - P^{m+1}_{1,2,3,4}; \\ (\sigma_{\theta\theta})^{m+1}_{1,2,3,4} &= (\bar{\sigma}_{\theta\theta})^{m+1}_{1,2,3,4} - P^{m+1}_{1,2,3,4}. \end{aligned}\right\} \tag{132}$$

The final calculation is the energy of the region of a check on the accuracy of the calculations. The internal energy added by zones is

$$(IE)^{m+1} = 2\Pi \sum_{I,J} E^{m+1}_{I,J}, m^0_{I,J}, \tag{133}$$

and the kinetic energy is

$$(KE)^{m+1} = \frac{\Pi}{4} \sum_{I,J} \left[\left(u^{m+1}_{I,J} \right)^2 + \left(w^{m+1}_{I,J} \right)^2 \right] \left(M^0_1 + M^0_2 + M^0_3 + M^0_4 \right). \tag{134}$$

This completes one cycle of calculation.

IV. SAMPLE PROBLEM

A. Reactor Configuration

Consider a typical LMFBR core of stainless steel-clad, oxide fuel pins supported in stainless steel grid plates and cooled by liquid sodium. As shown in Fig. 5, the core is surrounded by a radial blanket, an upper blanket and plenum, and a lower blanket, all immersed in the sodium coolant. The sodium is blanketed with argon gas and is contained in a steel vessel. This vessel is installed within a concrete cavity that has a rotating shield plug at the top. Also shown are the pertinent dimensions and Lagrangian meshes.

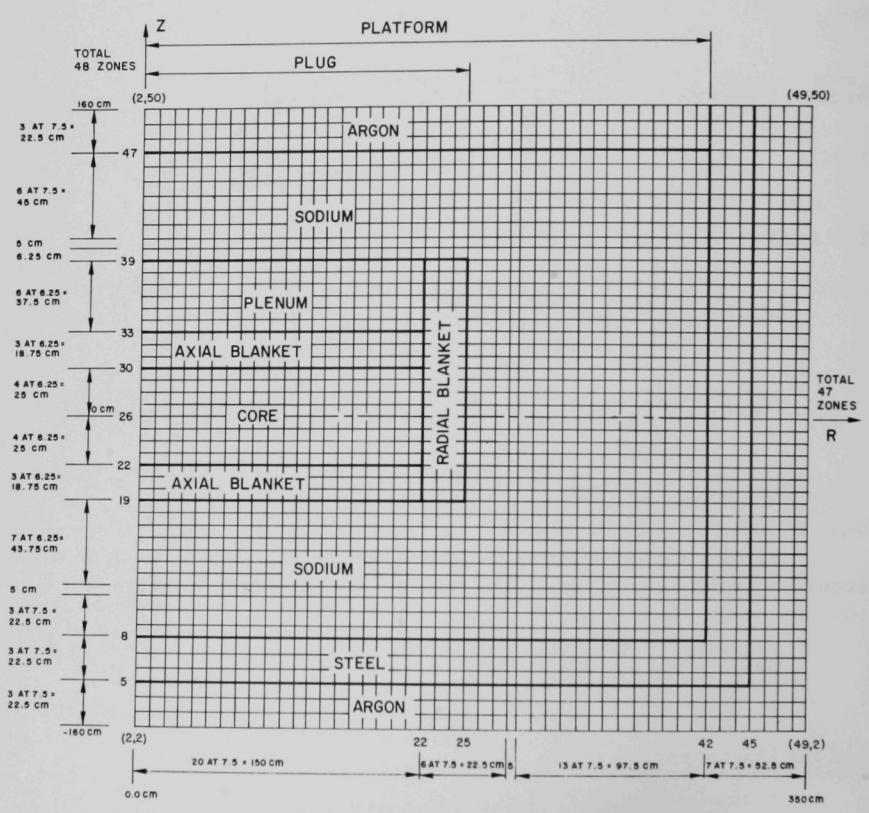

113-1942

Fig. 5. Lagrangian Grid for Sample Problem

B. Excursion Model

It is assumed that, at the start of the power excursion, the core is molten and the sodium has been vaporized and expelled from the core region, but the blankets are still intact. During the excursion, the energy release is so rapid that the molten oxide fuels are vaporized and superheated to a high temperature and pressure. At the end of the excursion, the core consists of high-pressure oxide vapor, surrounded by the blankets and liquid sodium in their preexcursion state.

The equation of state for the core oxide is assumed to have the form

$$p = B \exp\left(-\frac{C}{E + D}\right), \tag{135}$$

where p is the pressure, E is the internal energy, and B, C, and D are constants. The equations of state for the blankets, plenum, steel, and sodium are the Mie Grüneisen type,

$$P = P_H + \frac{\gamma}{v}(E - E_H), \tag{136}$$

where P_H and E_H are the pressure and internal energy, respectively, along the Hugoniot curve, γ is the Grüneisen coefficient, and v is the specific volume. The equation of state for argon is

$$p = \frac{(n - 1)E}{V},$$

where n is the isentropic coefficient. Values of B, C, D, γ, n, V, and P_H are read into the program inputs.

C. Results

Figure 6 shows the initial layout and time sequence of the Lagrangian grids. Pressure profiles along R(I) = 2 and Z(J) = 26 are shown in Figs. 7 and 8, respectively.

The computation was terminated at t = 808 μsec, when the force acting on the plug exceeded the strength of the plug holddown device. The total computer time is about 60 min.

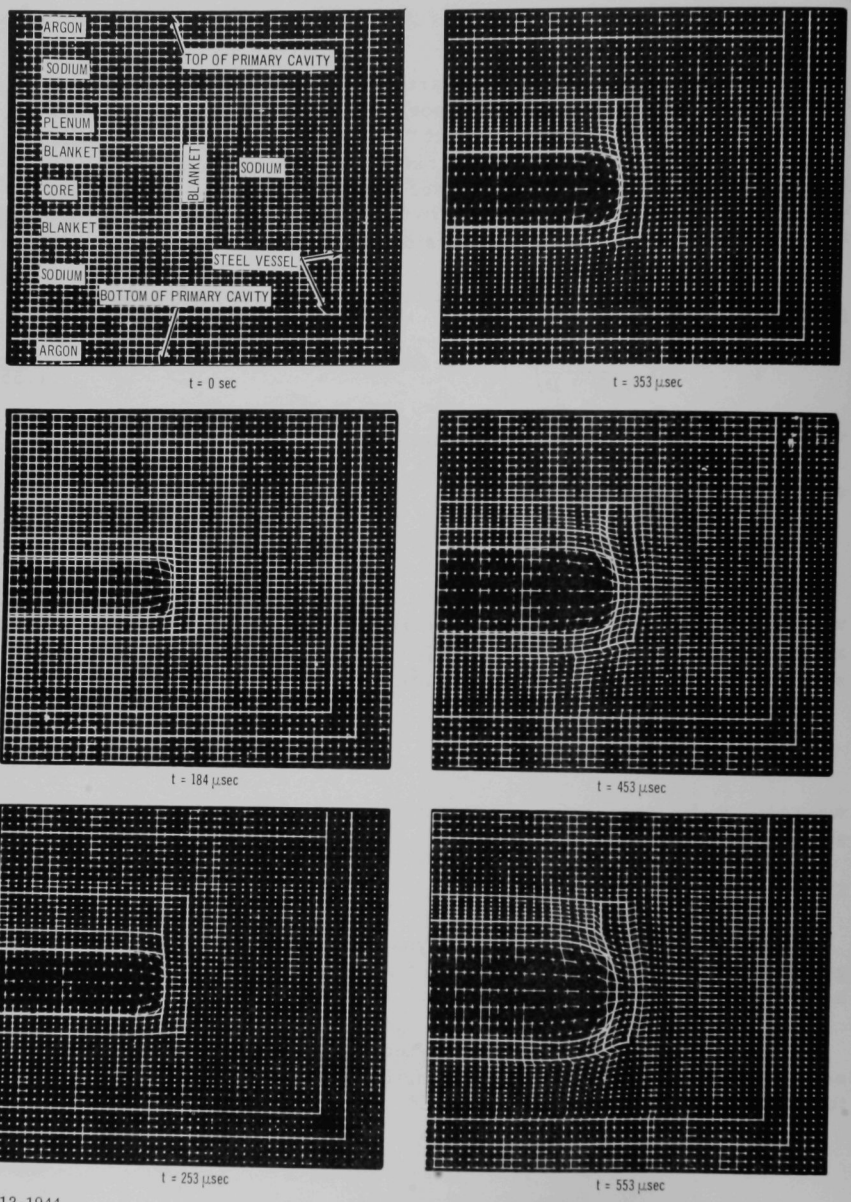

113-1944

Fig. 6. Deformation of Lagrangian Grids at Various Times after Start of a Power Excursion in a "Pancake" Core Configuration

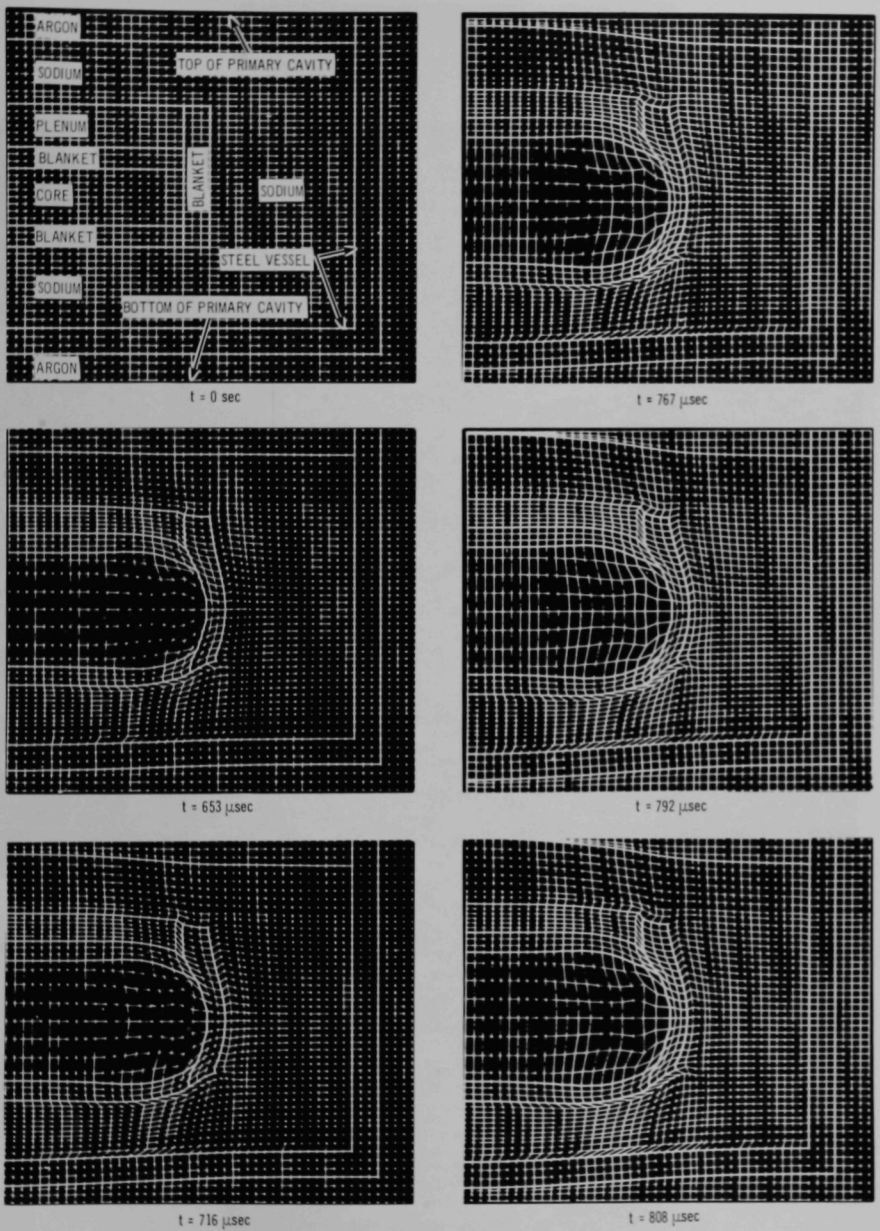

113-1932

Fig. 6. (Contd)

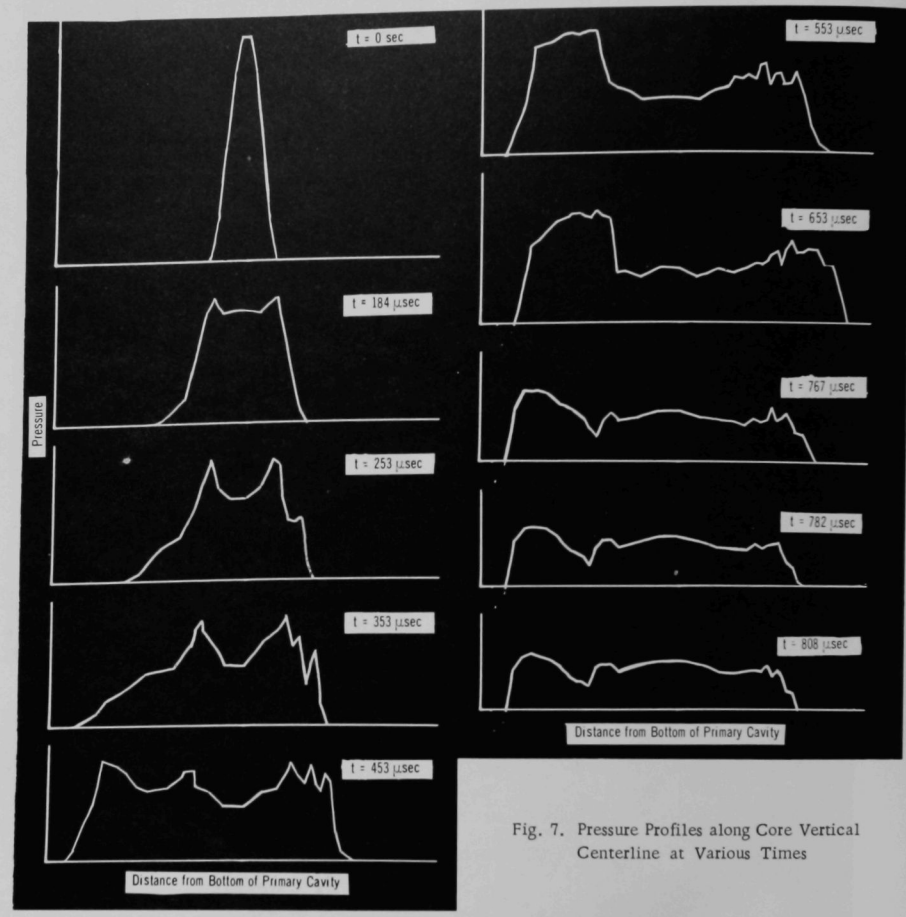

113-1933

Fig. 7. Pressure Profiles along Core Vertical Centerline at Various Times

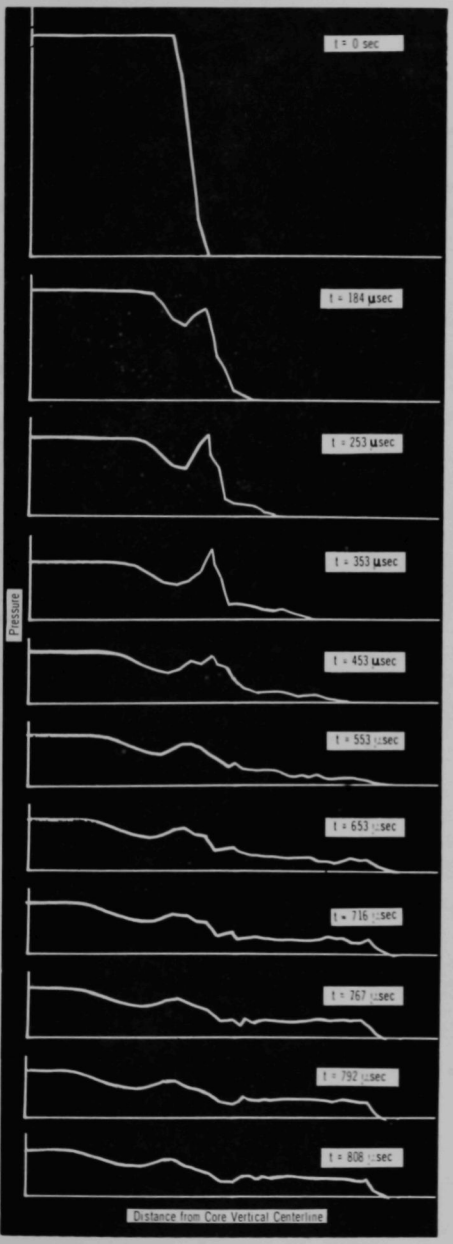

113-1934

Fig. 8. Pressure Profiles along Core Horizontal Axis at Various Times

APPENDIX A

Computer Program

1. Input Information Required

The following card types, which are required as input information to the program, are listed in the order in which they must appear in the data deck.

Card Type	Columns	Format	FORTRAN Name	Description
1	1-72	(18A4)	TITLE	Title card: 71 characters of alpha-numerics for problem identification. Column 1 must be blank.
2		(5I6,3F12.0)		
	1-6		IMAX	Number of zones in the radial (R) direction.
	7-12		JMAX	Number of zones in the axial (Z) direction.
	13-18		KB1	Boundary-condition indicator for the top surface (upper Z). KB1 = 0: Fixed surface KB1 = 1: Free surface
	19-24		KB2	Boundary-condition indicator for the cylindrical surface. KB2 = 0: Fixed surface KB2 = 1: Free surface
	25-30		KB3	Boundary-condition indicator for the bottom surface (lower Z). KB3 = 0: Fixed surface KB3 = 1: Free surface
	31-42		TIME	Initial problem starting time, in seconds.
	43-54		DELT	Initial time interval, in seconds.
	55-66		DELTM	Maximum time interval, in seconds.

Card Type	Columns	Format	FORTRAN Name	Description
3		(5F12.0)		
	1-12		CYCLM	Stop cycle. Allows the problem to be terminated after stop cycle. (If CYCLM = 0 or blank, the program sets CYCLM = 10000.)
	13-24		TMAX	Maximum time, in seconds. Allows the problem to be terminated after TMAX seconds. (If TMAX = 0 or blank, the program sets TMAX = 10000.)
	25-36		DISTM	Maximum distortion index. Allows the problem to be terminated if the distortion index, on any zone in the problem, exceeds DISTM. (If DISTM = 0 or blank, the program sets DISTM = 10000.)
	37-48		DE1	Instability warning indicator. If the percentage change in the total energy is greater than DE1, the program ignores IOUA instruction on card of type 4, and prints full-accuracy output every cycle. (If DE1 = 0 or blank, the program sets DE1 = 0.001.)
	49-60		DE2	Instability control parameter. Allows the problem to be terminated if the percentage change in the total energy from the initial total energy exceeds DE2. (If DE2 = 0 or blank, the program sets DE2 = 0.005.)
4		(12I6)		
	1-6		IOUA	Parameter to determine the full-accuracy printout. IOUA > 0: Full-accuracy output every IOUA cycle. IOUA = 0: No printout.

Card Type	Columns	Format	FORTRAN Name	Description
4 (Contd.)	7-12		INUMBA	Maximum number of full-accuracy printouts. After the number of full-accuracy printouts exceeds INUMBA, the program prints the full-accuracy printout for the last cycle only.
	13-18		IOUB	Parameter to determine the limited 2-dimensional (2-D) printout. IOUB > 0: Limited 2-D output every IOUB cycle. IOUB = 0: No printout.
	19-24		IOUC	Parameter to determine film output. (IBM 2280 Film Recorder Picture Display.) IOUC > 0: Film output every IOUC cycle. IOUC = 0: No film output.
	25-30		IOUT	Parameter to determine restart capability--usage of auxiliary tapes 8 and 9. IOUT = 0: Tapes 8 and 9 are not used. IOUT = 1: After the computation is terminated, the program writes the output data on a binary tape 8, so that the problem may be continued later. IOUT = 2: Continuation of the problem from a previous run. Program reads the input data from a binary tape 9. IOUT = 3: Program combines both. IOUT = 1 and IOUT = 2 capabilities: Program reads the input data from a binary tape 9 and also writes the output data on a binary tape 8 for later continuation.

Note: For IOUT = 2 and 3, the input to the program is on tape 9; thus cards of type 5 to 19 are omitted and only cards of type 1, 2, 3, 4, 20, 21, 22, 23, and 24 are required.

Card Type	Columns	Format	FORTRAN Name	Description
5		(8F9.0)		Initial grid dimensions--radial direction.
	1-9		R(2,2)	$R_{I,2}$; I = 2, 3, ..., n.
	10-18		R(3,2)	
	19-27		R(4,2)	
	Use as many cards of type 5 as required; n = IMAX + 2.			
6		(8F9.0)		Initial grid dimensions--axial direction.
	1-9		Z(2,2)	$Z_{2,J}$; J = 2, 3, ..., n.
	10-18		Z(2,3)	
	19-27		Z(2,4)	
	Use as many cards of type 6 as required; n = JMAX + 2.			
7	1-6	(I6)	NSEC	Number of rectangular sections into which the grid is subdivided.
8		(7I6,2F9.0)		Section cards.
	1-6		$KR1_k$	Starting zone number in the radial direction.
	7-12		$KR2_k$	Final zone number in the radial direction.
	13-18		$KZ1_k$	Starting zone number in the axial direction.
	19-24		$KZ2_k$	Final zone number in the axial direction.
	25-30		$KT1_k$	Material indicator. $KT1_k$ = 1 (core), 2 (sodium), 3 (steel), 4 (argon), 5 (axial blanket), 6 (radial blanket), 7 (plenum), 8 (water). As used in the sample problem.
	31-36		$KT2_k$	Material phase indicator. $KT2_k$ = 1 (solids or liquids), 2 (vapor).

Card Type	Columns	Format	FORTRAN Name	Description
8 (Contd.)	37-42		KTM_k	Parameter describing the types of input used for zone properties (ρ,E,P). $KTM_k = 1$: Input for all zones in this section is on cards of type 10. $KTM_k = 0$: Input for each zone in this section is on cards of type 14.
	43-51		RDD	Initial radial velocity, in cm/sec.
	52-60		ZDD	Initial axial velocity, in cm/sec.
9	1-6	(I6)	NMAT	Number of different materials. NMAT must be equal or greater than any $KT1_k$ on cards of type 8.
10		(6F9.0,I3)		
	1-9		AA_k	a: Constants for equation of state (gaseous materials): Core P = a exp[-b/(E+C)].
	10-18		BB_k	b: Constants for equation of state (gaseous materials): Core P = a exp[-b/(E+C)].
	19-27		CC_k	c: Constants for equation of state (gaseous materials): Core P = a exp[-b/(E+C)]. Argon P = aEρ. Used only when $KT2_k = 2$ for the same material.
	28-36		$CRHO_k$	Initial density ρ_0, in g/cm^3.
	37-45		CE_k	Initial energy E_0, in dyne-cm/g.
	46-54		CP_k	Initial pressure P_0, in dynes/cm^2.
	55-57		KKK_k	Number of PP_I and VV_I values on cards of type 12. PP_I and VV_I represent Hugoniot curve for the material. If $KKK_k \leq 0$, cards of type 12 are not used.
11		(6F9.0)		
	1-9		CWN_k	η: Constants for stability criterion (see Eq. 74).
	10-18		CWB_k	P_B: Constants for stability criterion (see Eq. 74).

Card Type	Columns	Format	FORTRAN Name		Description
11 (Contd.)	19-27		$CPLG_k$		The maximum allowable strain for the material. The problem will be terminated when the strain in any zone exceeds $CPLG_k$. If $CPLG_k \leq 0$, the calculation of strains and stresses for the material is omitted.
	28-36		CYO_k		Material yield strength in dynes/cm^2.
	37-45		CNU_k		Material Poisson's ratio.
	Note: CYO_k and CNU_k are used only when $CPLG_k > 0$.				
12		(8F9.0)			Hugoniot curve points. Used only when $KKK_k > 0$.
	1-9		$PP_{k,1}$	$(P_H)_1$	P_H are the pressure values in kilobars on Hugoniot curve for the specified material k. $(V/V_0)_1$ are the ratios of the specific volumes for the $(P_H)_I$ values. I = 1, 2, ..., KKK_k.
	10-18		$VV_{k,1}$	$(V/V_0)_1$	
	19-27		$PP_{k,2}$	$(P_H)_2$	
	28-36		$VV_{k,2}$	$(V/V_0)_2$	
	Use as many cards of type 12 as required: $0 < KKK \leq 50$. Note: The Hugoniot curves on cards are in increasing order of V/V_0.				
13		(8F9.0)			Constants for materials that are using the Hugoniot table. Used only when $KKK_k > 0$.
	1-9		PO_k		Initial pressure at which the Hugoniot curve is calculated, in dynes/cm^2.
	10-18		ROK		Initial density for the Hugoniot curve, in g/cm^3.
	19-27		EO_k		Initial specific energy for the Hugoniot curve, in dyne-cm/g.
	28-36		GO_k		γ_1: Mie-Grüneisen coefficient.
	37-45		CO_k		γ_2: Additional Mie-Grüneisen coefficient; used when material is steel for $P_H > 131$ kb, or water for $P_H > 136$ kb.

Card Type	Columns	Format	FORTRAN Name	Description
14		(2I3,7F9.0,2I3)		Card input for individual zones. Used only when $KTM_k = 0$ on card of type 8.
	1-3		$II_{I,J}$	Zone number in the radial direction.
	4-6		$JJ_{I,J}$	Zone number in the axial direction.
	7-15		$RC1_{I,J}$	Radial dimension, in cm.*
	16-24		$ZC1_{I,J}$	Axial dimension, in cm.*
	25-33		$RDOT_{I,J}$	Radial velocity, in cm/sec.*
	34-42		$ZDOT_{I,J}$	Axial velocity, in cm/sec.*
	43-51		$RHO_{I,J}$	Density, in g/cm^3.
	52-60		$E_{I,J}$	Specific energy, in dyne-cm/g.
	61-69		$P_{I,J}$	Pressure in dynes/cm^2.
	70-72		$KTX_{I,J}$	Material indicator; same identification as $KT1_k$ on card of type 8.
	73-75		$KTY_{I,J}$	Material phase indicator; same identification as $KT2_k$ on card of type 8.
15		(5I6,F12.0, 2I6,F12.0)		Parameters to describe the plug and platform calculations (upper surface).
	1-6		KPP	Parameter that determines whether platform motion is to be calculated. KPP = 1: Platform motion is calculated according to $M\ddot{Z} + CZ + K\dot{Z} = F(t)$, where M is the total mass of the platform,

* These values are the displacements and velocities at the lower left corner of the individual zone.

Note: When $KTM_k = 0$ on card of type 8, cards of type 14 must be entered in the following order for each section: First, cards having $J = KZ1_k$ arranged in the increasing order of I, i.e., from $1 = KR1_k$ to $1 = KR2_k$. Next, groups of cards having $J = KZ1_k + 1$, $KZ1_k + 2$, etc., until $J = KZ2_k$. In each group, cards are again arranged in increasing order of I, i.e., from $I = KR1_k$ to $I = KR2_k$. $KR1_k$, $KR2_k$, $KZ1_k$, and $KZ2_k$ are defined on cards of type 8.

Card Type	Columns	Format	FORTRAN Name	Description
15 (Contd.)	1-6		KPP (Contd.)	KZ is the spring force, $C\dot{Z}$ is the damping force, and F(t) is the total force applied by the system on the platform. KPP = 0: No platform calculations.
	7-12		KPP1	Radial zone number where the platform starts.
	13-18		KPP2	Radial zone number where the platform ends (KPP2 ≥ KPP1).
	19-24		KPPX	Number of CX_I and CXD_I values on cards of type 16, where the spring force KZ_I versus Z_J is tabulated. If KPPX < 0, KZ is set to zero.
	25-30		KPPC	Number of CV_I and CVD_I values on cards of type 17, where the damping force $C\dot{Z}_I$ versus $\dot{Z}_I$ is tabulated. If KPPC ≤ 0, CZ is set to zero.
	31-42		PMASS	Total mass of platform, in grams.
	Note: KPP1, KPP2, KPPX, and KPPC are used only when KPP = 1.			
	43-48		KPL1	Parameter to determine plug calculations. If KPL1 > 0, the total force applied by the system on the plug is calculated. KPL1 indicates the number of the first radial zone of the plug.
			KPL2	Number of the last radial zone of the plug (KPL2 ≥ KPL1).
			PLUG	Allowable plug force, in dynes. Problems will be terminated when the force acting on the plug exceeds PLUG.
	Note: KPL2 and PLUG are used only when KPL1 > 1.			

Card Type	Columns	Format	FORTRAN Name	Description
16		(8F9.0)		KZ_I versus Z_I table. Used only when KPPX > 0 on card of type 15.
	1-9		CX_1	KZ_1
	10-18		CXD_1	Z_1
	19-27		CX_2	KZ_2
	28-36		CXD_2	Z_2
				KZ_I is the spring force, in dynes, for the displacement Z_I, in cm.
	Use as many cards of type 16 as required.			
	Note: The KZ_I versus Z_I values are entered in pairs in increasing order of Z_I, starting with Z_1 (= 0), Z_2, ..., to Z_{KPPX}.			
17		(8F9.0)		$C\dot{Z}_I$ versus $\dot{Z}_I$ table. Used only when KPPC > 0 on card of type 15.
	1-9		CV_1	$C\dot{Z}_1$
	10-18		CVD_1	$\dot{Z}_1$
	19-27		CV_2	$C\dot{Z}_2$
	28-36		CVD_2	$\dot{Z}_2$
				$C\dot{Z}_I$ is the damping force, in dynes, for the velocity $\dot{Z}_I$, in cm/sec.
	Use as many cards of type 17 as required.			
	Note: The $C\dot{Z}_I$ versus $\dot{Z}_I$ values are entered in pairs in increasing order of $\dot{Z}_1$, starting with $\dot{Z}_1$ (= 0), $\dot{Z}_2$, ..., to $\dot{Z}_{KPPC}$.			
18	1-6	(I6)	NPP	Number of zones for which pressures and/or displacements are printed after each cycle. These values also may be displayed using the Calcomp option. (See card type 24.)
19	1-6	(12I6)	KXP_1	First radial zone number.
	7-12		KYP_1	First axial zone number.
	13-18		KXP_2	Second radial zone number.
	19-24		KYP_2	Second axial zone number.
	KXP_j and KYP_j define each zone to be displayed; j = 1, 2, ..., NPP ($0 \leq NPP \leq 6$). The signs before KXP_j and KYP_j indicate the type of information to be displayed.			

Card Type	Columns	Format	FORTRAN Name	Description
19 (Contd.)				$KXP_j > 0$, $KYP_j > 0$: Pressure
				$KXP_j < 0$, $KYP_j > 0$: Radial displacement of lower left corner.
				$KXP_j > 0$, $KYP_j < 0$: Axial displacement of lower left corner.

Note: Card type 19 is used only when NPP > 0.

The following cards are used only when IOUC > 0.

20	1-6	(I6)	N	Number of lines on the grid that are to be repeated to provide heavier outline for film output.
21		(12I6)		Specification of the lines that are to be repeated. Used only when N > 0 on card of type 20.
	1-6		$IX1_1$	Starting mesh-point number of the first line (in radial direction).
	7-12		$IX2_1$	Final mesh-point number of the first line (in radial direction).
	13-18		$JX1_1$	Starting mesh-point number of the first line (in axial direction).
	19-24		$JX2_1$	Final mesh-point number of the first line (in axial direction).
	25-30		$IX1_2$	Starting mesh-point number of the second line (in radial direction).

Use as many cards of type 21 as required, three lines per card.

Note: For each line J, either $IX1_J = IX2_J$ or $JX1_J = JX2_J$; $J = 1, 2, \ldots, N$ $(1 \leq N \leq 50)$.

Card Type	Columns	Format	FORTRAN Name	Description
22	1-6	(I6,F12.0)	NNM	Number of pressure curves for each displayed cycle.
	7-18		PMAX	Maximum pressure, in dynes/cm^2, that can be plotted.
23		(12I6)		Specification of the lines for which the pressure is plotted. Used only when NNM > 0 on card of type 22.
	1-6		$NX1_1$	For positive $NX1_i$, program plots the pressure for all axial zones (Z_J - J = 2, JMAX + 1) at the radial zone R = $NX1_i$. For negative $NX1_i$, program plots the pressure for all radial zones (R_I - I = 2, IMAX + 1) at the axial zone Z = $NX1_i$.
	7-12		$NX1_2$	
	13-18		$NX1_3$	

Use as many cards of type 23 as required, 12 numbers per card; i = 1, 2, ..., NMN (1 ≤ NN1 ≤ 50).

24		(I6,(6F12.0))		Calcomp option card.
	1-6		KCAL	KCAL > 0: Program draws Calcomp plots of plug force and the values specified on cards of types 18 and 19 versus time. KCAL ≤ 0: No Calcomp plot.
	7-18		SCT	Scale for time axis (horizontal). SCT is the number of seconds per inch of plot. If SCT = 0.0 or blank, the program sets SCT = 0.001.
	19-30		SCT1	Scale for plug force (vertical axis). SCT1 is the number of dynes per inch of plot. If SCT1 = 0.0 or blank, the program calculates the optimum scale.
	31-42		$SCTK_1$	Scale for first value described on input cards of types 18 and 19 (vertical axis). If $SCTK_1$ = 0.0 or blank, the program calculates the optimum scale.
	43-45		$SCTK_2$	

Use as many cards as required; K = 1, 2, ..., NPP (0 ≤ NPP ≤ 6).

2. Computer Output

a. Standard Program Printout

(1) Title of problem

(2) Input data

(3) Total energy

(4) For each cycle:

(a) Full-accuracy output (see Subsection a(1) below)

(b) Limited 2-D output (see Subsection a(2) below)

(c) Time (sec); total internal energy (dyne-cm); total kinetic energy (dyne-cm); and total energy (dyne-cm)

(d) Cycle number; time; time interval (D-TIME); maximum distortion index (DISTORT); location of the maximum distorted zone; maximum (calculated) White stability number (WMAX) and its location

(e) Plug force and other values requested on input cards of types 18 and 19. (These values are also printed at the end of each run.)

(5) Reason for termination of run (if other than specified on input card type 3).

(1) Full Accuracy Output. When IOUA > 0, a full-accuracy printout is given for each IOUA cycle, subject to the limitation in INUMBA. (See input card type 4 for explanation of IOUA and INUMBA.)

(a) For each cycle

i. Title of problem

ii. Cycle number

iii. Time.

(b) For each zone

Eleven columns, consisting of integers I and J; $R_{I,J}$; $Z_{I,J}$; $\dot{R}_{I,J}$; $\dot{Z}_{I,J}$; $P_{I,J}$; $VP_{I,J}$; $E_{I,J}$; $\rho_{I,J}$; and material and phase indicators.

$R_{I,J}$, $Z_{I,J}$ = position of lower left corner of zone I,J (in cm),

$\dot{R}_{I,J}$, $\dot{Z}_{I,J}$ = velocity of lower left corner of zone I,J (in cm/sec),

$P_{I,J}$ = total pressure (in dynes/cm^2),

$VP_{I,J}$ = viscous pressure (in dynes/cm^2),

$E_{I,J}$ = internal energy (in dyne-cm/g),

and

$\rho_{I,J}$ = density (in g/cm^3).

Note: For the initial data (cycle = 0), $M^0_{I,J}$ is printed instead of $VP_{I,J}$, where $M^0_{I,J}$ is the mass (in grams) of each zone.

(2) Limited 2-D Output. This integer output is printed for every IOUB cycle only when IOUB > 0. It is in the form of a matrix and includes the following properties:

(a) Initial radial position of the grid points ($R^0_{I,J}$)

(b) Initial axial position of the grid points ($Z^0_{I,J}$)

Note: Items a and b are printed only when cycle number = 0.

(c) Radial displacement of the grid points from the initial position.

(d) Axial displacement of the grid points from the initial position

(e) Radial velocity of the grid points

(f) Axial velocity of the grid points

(g) Total pressure of the zones

(h) Viscous pressure of the zones

(i) Specific internal energy of the zones

(j) Density of the zones

(k) Radial strain of the zones

(l) Axial strain of the zones

(m) Angular strain of the zones

(n) Shear strain of the zones

(o) Radial stresses of the zones

(p) Axial stresses of the zones

(q) Angular stresses of the zones

(r) Shear stresses of the zones.

More specifically, each page of printout is prefaced by the problem title, property definition, time, time interval, cycle number, maximum absolute value, and scale factor used. This is followed by a matrix (maximum 50 x 25) of the property values, where the rows indicate radial direction and the columns indicate axial direction. Numbers are printed on the top and left side of the matrix to indicate the position of each zone in the grid. If the grid size exceeds 50 x 25, the printout continues on successive pages until the grid is completed.

To obtain the printed integers, the program multiplies the calculated property values by the indicated scale factor and then truncates. The maximum number of integers for each property is limited to 4; thus the maximum number printed is ±9999. If all calculated values are zeros, the matrix output is omitted.

b. Pictorial Display (IBM-2280 Film Recorder)

Pictorial displays of the grid displacement and pressure can be obtained for every IOUC cycle only when IOUC > 0. (See input card type 4.)

(1) Grid Displacement. The program draws the grids for specified cycles according to the input on cards of type 20 and 21, and then obtains the required film output. Cycle number and time (in seconds) are drawn at the top of each grid. Note: The lower left corner of the picture indicates the position of $R_{2,2}$ and $Z_{2,2}$.

(2) Pressure. If a pressure display in either the axial or radial direction is specified, the program plots the pressure of each zone (at the lower zone mesh point) in the specified direction, and then draws the interconnecting vectors. Note: The zone number in the other direction is constant.

To ensure uniform scaling of the plots, the expected maximum pressure must be specified. (See input cards of type 22 and 23.)

c. Calcomp Display

This display is executed at the end of a problem, but only when KCAL > 0. (See input card type 24.)

When executed, the program plots, as a function of time elapsed, the total force applied on the plug by the system. It also plots, as a function of time, the values described on input cards of types 18 and 19.

Each of the above plots has its own vertical and horizontal axis. The latter always represents time, and its scale is specified on input

card type 24. Scales for the vertical axis (10 in. are allowed) may be specified on card type 24; if not, the program finds the optimum scale from the calculated values. On all plots, consecutive points are interconnected with vectors.

3. Program Limitations and Subroutines

a. Limitations

Number of:	Not to exceed:
(1) Grid zones	3000
(2) Different materials	20
(3) Different sections	20
(4) Points for Hugoniot curve(s)	50
(5) Points for KZ vs Z and $\dot{CZ}$ vs $\dot{Z}$ tables	50
(6) Lines repeated for pictorial display	50
(7) Different pressure plots/cycle	50
(8) Reactor vessels	10
(9) Points for stress vs strain table for reactor material	50
(10) Cycles/run for Calcomp display	1000
(11) Different plots for Calcomp display	7

b. Subroutines

To execute the pictorial display, the program uses the subroutines described in:

A Film-Plotting Subroutine Package (FSP) for the IBM Film Recorder, by Daniel F. Carson (Argonne AMD Technical Memorandum No. 167, June 17, 1968).

To execute the Calcomp display, the program uses the subroutines described in:

S/360 Programming Techniques for the Calcomp 780, by Ronald F. Krupp (Argonne AMD Technical Memorandum No. 130, January 6, 1967).

APPENDIX B

Conservation Laws for 2-D Axisymmetric Shock Wave Propagation

In this appendix, we derive the basic conservation laws of mass, momentum, and energy, along with the equation of state.

1. Conservation of Mass

a. Incremental Form

$$\rho d\forall = \rho^0 d\forall^0, \tag{B.1}$$

where

$\rho, d\forall$ = density and incremental volume change, respectively, at time $t > 0$;

and

$\rho^0, d\forall^0$ = density and undeformed incremental volume, respectively, at time $t = 0$.

b. Tensor Differential Form

The tensor equation is

$$\frac{d\rho}{dt} + \rho d^i_i = 0. \tag{B.2}$$

Now,

$$d^i_j = d_{ij} = u,^i_j = \dot{x}^i_j, \tag{B.3}$$

where u, and x are the velocity and displacement, respectively, and conventional tensor notation prevails. On using Eq. B.3, Eq. B.2 becomes

$$\dot{\rho} + \rho u,^i_i = 0. \tag{B.4}$$

For cylindrical coordinates, the three principal coordinates are

$$i = r, \theta, z, \tag{B.5}$$

and the three velocities are

$$u = u, v, w. \tag{B.6}$$

On using Eq. B.5, Eq. B.4 becomes

$$\dot{\rho} + \rho\left(\frac{\partial u}{\partial r} + \frac{\partial v}{\partial \theta} + \frac{\partial w}{\partial z}\right) = 0. \tag{B.7}$$

c. Physical-coordinate Differential Form

To obtain the conservation of mass in physical coordinates, the velocity tensor is needed, which is

$$u,^{i}_{j} = \frac{\partial(u, v, w)}{\partial(r, \theta, z)} = \begin{bmatrix} \frac{\partial u}{\partial r} & 0 & \frac{\partial u}{\partial z} \\ 0 & \frac{u}{r} & 0 \\ \frac{\partial w}{\partial r} & 0 & \frac{\partial w}{\partial z} \end{bmatrix}. \tag{B.8}$$

On using Eq. B.8, Eq. B.7 becomes

$$\dot{\rho} + \rho\left(\frac{\partial u}{\partial r} + \frac{u}{r} + \frac{\partial w}{\partial z}\right) = 0. \tag{B.9}$$

2. Conservation of Momentum

a. Tensor Differential Form

The basic equation of momentum is

$$\rho \dot{u}^{i} = \rho f^{i} + t,^{im}_{m} \qquad (i, m = r, \theta, z), \tag{B.10}$$

where

f^{i} = body force

and

t^{im} = symmetric stress tensor.

The stress tensor is defined as

$$\| t^{im} \| = \begin{bmatrix} \sigma_{rr} & \sigma_{r\theta} & \sigma_{rz} \\ \sigma_{\theta r} & \sigma_{\theta\theta} & \sigma_{\theta z} \\ \sigma_{zr} & \sigma_{z\theta} & \sigma_{zz} \end{bmatrix}. \tag{B.11}$$

Equation B.11 can be rewritten as the sum of a hydrostatic and deviatoric stress tensor as follows:

$$\| t^{im} \| = \begin{bmatrix} P & 0 & 0 \\ 0 & P & 0 \\ 0 & 0 & P \end{bmatrix} + \begin{bmatrix} \bar{\sigma}_{rr} & \sigma_{r\theta} & \sigma_{rz} \\ \sigma_{\theta r} & \bar{\sigma}_{\theta\theta} & \sigma_{\theta z} \\ \sigma_{zr} & \sigma_{z\theta} & \bar{\sigma}_{zz} \end{bmatrix}, \tag{B.12}$$

where

$$P = -\tfrac{1}{3}(\sigma_{rr} + \sigma_{\theta\theta} + \sigma_{zz}), \tag{B.13}$$

$$\bar{\sigma}_{rr} = \sigma_{rr} + P, \tag{B.14}$$

$$\bar{\sigma}_{\theta\theta} = \sigma_{\theta\theta} + P = -(\bar{\sigma}_{rr} + \bar{\sigma}_{zz}), \tag{B.15}$$

$$\bar{\sigma}_{zz} = \sigma_{zz} + P, \tag{B.16}$$

and

$$\bar{\sigma}_{ij} = \sigma_{ij} \quad (i \neq j). \tag{B.17}$$

On using Eqs. B.12-B.17, we can write the stress tensor as

$$t^{im} = \frac{1}{3} t^i_i \delta^i_j + {}^d t^{im}, \tag{B.18}$$

where δ^i_j is the Kronecker delta. Next, let

$$P = -\frac{1}{3} t^i_i. \tag{B.19}$$

Then, Eq. B.18 becomes

$$t^{im} = -(P\delta^i_i)^m + {}^d t^{im}. \tag{B.20}$$

On using Eq. B.20, the momentum equation (Eq. B.19) becomes

$$\rho u^i = \rho f^i - (P\delta^i_j)^{,m}_{,m} + {}^d t^{im}_{,m}. \tag{B.21}$$

b. Physical Equations of Motion

Based upon the tensor form in Eqs. B.10 and B.11, the momentum equations are

$$\rho\ddot{r} = \rho\dot{u} = \frac{\partial\sigma_{rr}}{\partial r} + \frac{\partial\sigma_{rz}}{\partial z} + \frac{\sigma_{rr} - \sigma_{\theta\theta}}{r} + \rho f^{r} \tag{B.22}$$

and

$$\rho\ddot{z} = \rho\dot{w} = \frac{\partial\sigma_{zz}}{\partial z} + \frac{\partial\sigma_{rz}}{\partial r} + \frac{\sigma_{rz}}{r} + \rho f^{z}. \tag{B.23}$$

Based upon the tensor form in Eqs. B.12 and B.20, the momentum equations become

$$\rho\ddot{r} = \rho\dot{u} = -\frac{\partial P}{\partial r} + \frac{\partial\bar{\sigma}_{rr}}{\partial r} + \frac{\partial\sigma_{rz}}{\partial z} + \frac{\bar{\sigma}_{rr} - \bar{\sigma}_{\theta\theta}}{r} + \rho f^{r} \tag{B.24}$$

and

$$\rho\ddot{z} = \rho\dot{w} = -\frac{\partial P}{\partial z} + \frac{\partial\bar{\sigma}_{zz}}{\partial z} + \frac{\partial\sigma_{rz}}{\partial r} + \frac{\sigma_{rz}}{r} + \rho f^{z}. \tag{B.25}$$

On using Eq. B.13, Eqs. B.24 and B.25 become

$$\rho\ddot{r} = \rho\dot{u} = -\frac{\partial(P - \bar{\sigma}_{rr})}{\partial r} + \frac{\partial\sigma_{rz}}{\partial z} + \frac{2\bar{\sigma}_{rr} + \bar{\sigma}_{zz}}{r} + \rho f^{r} \tag{B.26}$$

and

$$\rho\ddot{z} = \rho\dot{w} = -\frac{\partial(P - \bar{\sigma}_{zz})}{\partial z} + \frac{\partial\sigma_{rz}}{\partial r} + \frac{\sigma_{rz}}{r} + \rho f^{z}. \tag{B.27}$$

3. Conservation of Internal Energy

a. Tensor Form

The basic equation is

$$\rho\dot{E} = t^{im}d_{im} + h,^{i}_{i} + \rho Q \qquad (i, m = r, \theta, z), \tag{B.28}$$

where

E, h, Q = internal energy, heat-flux vector, and energy sources, respectively.

On using Eq. B.18, we obtain

$$t^{im}d_{im} = \frac{1}{3}t^{i}_{i}d^{i}_{i} + d_{t}{}^{im}\, d_{d_{im}}, \tag{B.29}$$

which, on using Eq. B.19, becomes

$$t^{im}d_{im} = -Pd^i_i + {}^{d}t^{im}\,{}^{d}d_{im}. \tag{B.30}$$

From Eq. B.2,

$$d^i_i = -\frac{\dot{\rho}}{\rho}, \tag{B.31}$$

which, on substitution in Eq. B.30, yields

$$t^{im}d_{im} = P\frac{\dot{\rho}}{\rho} + {}^{d}t^{im}\,{}^{d}d_{im}. \tag{B.32}$$

Next, using Eq. B.32, Eq. B.28 becomes

$$\rho\dot{E} = P\frac{\dot{\rho}}{\rho} + {}^{d}t^{im}\,{}^{d}d_{im} + h,^i_i + \rho Q. \tag{B.33}$$

Now, ${}^{d}d_{im}$ can be written as

$${}^{d}d_{im} = {}^{d}d^i_m = d^i_m - \frac{1}{3}d^i_i\delta^i_m = d^i_m + \frac{1}{3}\frac{\dot{\rho}}{\rho}\delta^i_m, \tag{B.34}$$

so that Eq. B.33 becomes

$$\rho\dot{E} = P\frac{\dot{\rho}}{\rho} + {}^{d}t^{im}d^i_m + \frac{1}{3}\frac{\dot{\rho}}{\rho}\,{}^{d}t^{im}\delta^i_m + h,^i_i + \rho Q. \tag{B.35}$$

b. Physical Equation Form

On using Eqs. B.2 and B.12, the components of ${}^{d}t^{im}\,{}^{d}d_{im}$ are

$${}^{d}t^{im}\,{}^{d}d_{im} = \begin{bmatrix} \frac{\partial u}{\partial r} + \frac{1}{3}\frac{\dot{\rho}}{\rho} & 0 & \frac{1}{2}\left(\frac{\partial u}{\partial z} + \frac{\partial w}{\partial r}\right) \\ 0 & \frac{u}{r} + \frac{1}{3}\frac{\dot{\rho}}{\rho} & 0 \\ \frac{1}{2}\left(\frac{\partial u}{\partial z} + \frac{\partial w}{\partial r}\right) & 0 & \frac{\partial w}{\partial z} + \frac{1}{3}\frac{\dot{\rho}}{\rho} \end{bmatrix} \tag{B.36}$$

Substitution of these components in Eq. B.35 gives

$$\rho E = P\frac{\dot{\rho}}{\rho} + \bar{\sigma}_{rr}\left(\frac{\partial u}{\partial \theta} + \frac{1}{3}\frac{\dot{\rho}}{\rho}\right) + \bar{\sigma}_{\theta\theta}\left(\frac{u}{r} + \frac{1}{3}\frac{\dot{\rho}}{\rho}\right) + \bar{\sigma}_{zz}\left(\frac{\partial w}{\partial z} + \frac{1}{3}\frac{\dot{\rho}}{\rho}\right)$$

$$+ \sigma_{rz}\left(\frac{\partial u}{\partial z} + \frac{\partial w}{\partial r}\right) + \left(\frac{\partial h^r}{\partial r} + \frac{h^r}{r} + \frac{\partial h^z}{\partial z}\right) + \rho Q. \qquad \text{(B.37)}$$

Now,

$$\rho = \frac{1}{v}, \qquad \text{(B.38)}$$

where v is the specific volume.

Differentiating Eq. B.38 with respect to time gives

$$\frac{\dot{\rho}}{\rho} = -\frac{\dot{v}}{v} = -\rho\dot{v}, \qquad \text{(B.39)}$$

which, on substitution in Eq. B.37, yields

$$\dot{E} = -P\dot{v} + v\left[\bar{\sigma}_{rr}\frac{\partial u}{\partial r} + \bar{\sigma}_{\theta\theta}\frac{u}{r} + \bar{\sigma}_{zz}\frac{\partial w}{\partial z} + \sigma_{rz}\left(\frac{\partial u}{\partial z} + \frac{\partial w}{\partial r}\right)\right]$$

$$- \frac{1}{3}\left(\bar{\sigma}_{rr} + \bar{\sigma}_{\theta\theta} + \bar{\sigma}_{zz}\right)\dot{v} + v\left(\frac{\partial h^r}{\partial r} + \frac{h^r}{r} + \frac{\partial h^z}{\partial z}\right) + Q. \qquad \text{(B.40)}$$

From Eqs. B.13-B.16,

$$\frac{1}{3}\left(\bar{\sigma}_{rr} + \bar{\sigma}_{\theta\theta} + \bar{\sigma}_{zz}\right) = 0, \qquad \text{(B.41)}$$

so that Eq. B.40 reduces to

$$\dot{E} = -P\dot{v} + v\left[\bar{\sigma}_{rr}\frac{\partial u}{\partial r} + \bar{\sigma}_{\theta\theta}\frac{u}{r} + \bar{\sigma}_{zz}\frac{\partial w}{\partial z} + \sigma_{rz}\left(\frac{\partial u}{\partial z} + \frac{\partial w}{\partial r}\right)\right]$$

$$+ v\left(\frac{\partial h^r}{\partial r} + \frac{h^r}{r} + \frac{\partial h^z}{\partial z}\right) + Q. \qquad \text{(B.42)}$$

At this point, it is convenient to introduce the strain rates defined as

$$\dot{\epsilon}_{rr} = \frac{\partial u}{\partial r}; \quad \dot{\epsilon}_{zz} = \frac{\partial w}{\partial z}; \qquad \text{(B.43)}$$

$$\dot{\epsilon}_{\theta\theta} = \frac{u}{r}; \quad \dot{\epsilon}_{rz} = \frac{\partial w}{\partial z} + \frac{\partial w}{\partial r}. \tag{B.44}$$

Thus, Eq. B.42 becomes

$$\dot{E} = -P\dot{v} + v\left(\bar{\sigma}_{rr}\dot{\epsilon}_{rr} + \bar{\sigma}_{\theta\theta}\dot{\epsilon}_{\theta\theta} + \bar{\sigma}_{zz}\dot{\epsilon}_{zz} + \sigma_{rz}\dot{\epsilon}_{rz}\right) + v\left(\frac{\partial h^r}{\partial r} + \frac{h^r}{r} + \frac{\partial h^z}{\partial z}\right) + Q. \tag{B.45}$$

4. Equation of State

Since no known equation of state prevails for all materials, the form assumed for each material is

$$p = p(E,v) = p(E,\rho). \tag{B.46}$$

APPENDIX C

Finite-difference Equations of the Jacobians

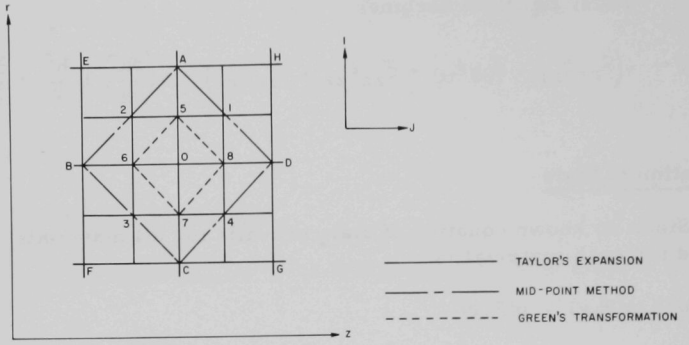

Finite-difference equations will be derived by all three methods. The correspondence between the letters and numbers in the illustration with Lagrangian coordinates is

	0 = I, J
1 = I + 1/2, J + 1/2	A = I + 1, J
2 = I + 1/2, J - 1/2	B = I, J - 1
3 = I - 1/2, J - 1/2	C = I - 1, J
4 = I - 1/2, J + 1/2	D = I, J + 1
5 = I + 1/2, J	E = I + 1, J - 1
6 = I, J - 1/2	F = I - 1, J - 1
7 = I - 1/2, J	G = I - 1, J + 1
8 = I, J + 1/2	H = I + 1, J + 1

Accelerations, velocities, and displacements are centered at the mesh point (0, A, B, C, D, E, F, G, H) and subscripted (I, J). Specific values of volume, pressure, area, viscosity, stresses, density, mass, and internal energy are centered at the middle of the zones (1, 2, 3, 4) and subscripted ($I \pm 1/2$, $J \pm 1/2$). Time is denoted by the superscript n.

To obtain the finite-difference form of the conservation laws the finite-difference form of the Jacobian for an arbitrary function F must be determined first.

$$\left.\frac{\partial(F, r)}{\partial(I, J)}\right|_0 = \left(\frac{\partial F}{\partial I}\right)_0\left(\frac{\partial r}{\partial J}\right)_0 - \left(\frac{\partial F}{\partial J}\right)_0\left(\frac{\partial r}{\partial I}\right)_0 = -A_0 \left.\frac{\partial F}{\partial z}\right|_0 \qquad \text{(C.1)}$$

$$\left.\frac{\partial(F, z)}{\partial(I, J)}\right|_0 = \left(\frac{\partial F}{\partial I}\right)_0\left(\frac{\partial z}{\partial J}\right)_0 - \left(\frac{\partial F}{\partial J}\right)_0\left(\frac{\partial z}{\partial I}\right)_0 = A_0 \left.\frac{\partial F}{\partial r}\right|_0 \qquad \text{(C.2)}$$

To find the values of the Jacobians in Eqs. C.1 and C.2 at the point 0, the partial derivatives at 0 must be evaluated for all three methods.

1. Taylor's Expansion

To evaluate the partial derivatives in Eqs. C.1 and C.2 by Taylor's method, centered differences will be used. Accordingly,

$$\left(\frac{\partial F}{\partial I}\right)_0 = \tfrac{1}{2}[(F_1 + F_2) - (F_3 + F_4)]; \tag{C.3}$$

$$\left(\frac{\partial F}{\partial J}\right)_0 = \tfrac{1}{2}[(F_1 + F_4) - (F_2 + F_3)]; \tag{C.4}$$

$$\left(\frac{\partial r}{\partial I}\right)_0 = \tfrac{1}{2}[(r_1 + r_2) - (r_3 + r_4)]; \tag{C.5}$$

$$\left(\frac{\partial r}{\partial J}\right)_0 = \tfrac{1}{2}[(r_1 + r_4) - (r_2 + r_3)]; \tag{C.6}$$

$$\left(\frac{\partial z}{\partial I}\right)_0 = \tfrac{1}{2}[(z_1 + z_2) - (z_3 + z_4)]; \tag{C.7}$$

$$\left(\frac{\partial z}{\partial J}\right)_0 = \tfrac{1}{2}[(z_1 + z_4) - (z_2 + z_3)]. \tag{C.8}$$

On using Eqs. C.3-C.8, Eqs. C.1 and C.2 become

$$\left.\frac{\partial(F, r)}{\partial(I, J)}\right|_0 = \tfrac{1}{4}[(F_1 - F_3 + F_2 - F_4)(r_1 - r_2 + r_4 - r_3) - (F_1 - F_2 + F_4 - F_3)(r_1 - r_3 + r_2 - r_4)] \tag{C.9}$$

and

$$\left.\frac{\partial(F, z)}{\partial(I, J)}\right|_0 = \tfrac{1}{4}[(F_1 - F_3 + F_2 - F_4)(z_1 - z_2 + z_4 - z_3) - (F_1 - F_2 + F_4 - F_3)(z_1 - z_3 + z_2 - z_4)]. \tag{C.10}$$

Multiplying out Eqs. C.9 and C.10 gives

$$\left.\frac{\partial(F, r)}{\partial(I, J)}\right|_0 = \tfrac{1}{2}[(F_2 - F_4)(r_1 - r_3) - (F_1 - F_3)(r_2 - r_4)] \tag{C.11}$$

and

$$\left.\frac{\partial(F, z)}{\partial(I, J)}\right|_0 = \tfrac{1}{2}[(F_2 - F_4)(z_1 - z_3) - (F_1 - F_3)(z_2 - z_4)]. \tag{C.12}$$

From Eqs. C.1 and C.2,

$$\left.\frac{\partial F}{\partial r}\right|_0 = \frac{1}{2A_0}[(F_2 - F_4)(z_1 - z_3) - (F_1 - F_3)(z_2 - z_4)] \tag{C.13}$$

and

$$\left.\frac{\partial F}{\partial z}\right|_0 = -\frac{1}{2A_0}[(F_2 - F_4)(r_1 - r_3) - (F_1 - F_3)(r_2 - r_4)]. \tag{C.14}$$

Using Eq. C.12 gives

$$A_0 = \left.\frac{\partial(r, z)}{\partial(I, J)}\right|_0 = \tfrac{1}{2}[(r_2 - r_4)(z_1 - z_3) - (r_1 - r_3)(z_2 - z_4)]. \tag{C.15}$$

Since the displacements are defined only at the mesh points, the values of the displacements in Eqs. C.5-C.15 must be regarded as the centroids of the mesh zones. Hence, to express these equations in terms of mesh points, we use the following relationships:

$$\left.\begin{aligned} r_1 &= \tfrac{1}{4}(r_0 + r_D + r_H + r_A); \\ r_2 &= \tfrac{1}{4}(r_0 + r_A + r_E + r_B); \\ r_3 &= \tfrac{1}{4}(r_0 + r_B + r_F + r_C); \\ r_4 &= \tfrac{1}{4}(r_0 + r_C + r_G + r_D); \end{aligned}\right\} \tag{C.16}$$

and

$$\left.\begin{aligned} z_1 &= \tfrac{1}{4}(z_0 + z_D + z_H + z_A); \\ z_2 &= \tfrac{1}{4}(z_0 + z_A + z_E + z_B); \\ z_3 &= \tfrac{1}{4}(z_0 + z_B + z_F + z_C); \\ z_4 &= \tfrac{1}{4}(z_0 + z_C + z_G + z_D); \end{aligned}\right\} \tag{C.17}$$

which yield the final equations

$$\left.\frac{\partial(F, r)}{\partial(I, J)}\right|_0 = \tfrac{1}{8}[(F_2 - F_4)(r_A - r_C + r_D - r_B + r_H - r_F)$$

$$- (F_1 - F_3)(r_A - r_C + r_B - r_D + r_E - r_G)] \qquad \text{(C.18)}$$

and

$$\left.\frac{\partial(F, z)}{\partial(I, J)}\right|_0 = \tfrac{1}{8}[(F_2 - F_4)(z_A - z_C + z_D - z_B + z_H - z_F)$$

$$- (F_1 - F_3)(z_A - z_C + z_B - z_D + z_E - z_G)]. \qquad \text{(C.19)}$$

2. Midpoint Method

The results for this case can be obtained from Section 1 of Appendix B by using the identities

$$\left.\begin{array}{l} 1 \to 5 \\ 2 \to 6 \\ 3 \to 7 \\ 4 \to 8 \end{array}\right\} \qquad \text{(C.20)}$$

in Eqs. C.11-C.15. Thus,

$$\left.\frac{\partial(F, r)}{\partial(I, J)}\right|_0 = \tfrac{1}{2}[(F_6 - F_8)(r_5 - r_7) - (F_5 - F_7)(r_6 - r_8)]; \qquad \text{(C.21)}$$

$$\left.\frac{\partial(F, z)}{\partial(I, J)}\right|_0 = \tfrac{1}{2}[(F_6 - F_8)(z_5 - z_7) - (F_5 - F_7)(z_6 - z_8)]; \qquad \text{(C.22)}$$

$$A_0 = \tfrac{1}{2}[(r_6 - r_8)(z_5 - z_7) - (r_5 - r_7)(z_6 - z_8)]; \qquad \text{(C.23)}$$

$$\left.\frac{\partial F}{\partial r}\right|_0 = \frac{1}{2A_0}[(F_6 - F_8)(z_5 - z_7) - (F_5 - F_7)(z_6 - z_8)]; \qquad \text{(C.24)}$$

$$\left.\frac{\partial F}{\partial z}\right|_0 = -\frac{1}{2A_0}[(F_6 - F_8)(r_5 - r_7) - (F_5 - F_7)(r_6 - r_8)]. \qquad \text{(C.25)}$$

Since the value of F must be known at the center of the zones and the coordinates at the mesh points, the definitions

$$\left.\begin{aligned} F_5 &= \tfrac{1}{2}(F_1 + F_2) \\ F_6 &= \tfrac{1}{2}(F_2 + F_3) \\ F_7 &= \tfrac{1}{2}(F_3 + F_4) \\ F_8 &= \tfrac{1}{2}(F_1 + F_4) \end{aligned}\right\}, \tag{C.26}$$

$$\left.\begin{aligned} r_5 &= \tfrac{1}{2}(r_0 + r_A); \quad r_6 = \tfrac{1}{2}(r_0 + r_B) \\ r_7 &= \tfrac{1}{2}(r_0 + r_C); \quad r_8 = \tfrac{1}{2}(r_0 + r_D) \end{aligned}\right\}, \tag{C.27}$$

and

$$\left.\begin{aligned} z_5 &= \tfrac{1}{2}(z_0 + z_A); \quad z_6 = \tfrac{1}{2}(z_0 + z_B) \\ z_7 &= \tfrac{1}{2}(z_0 + z_C); \quad z_8 = \tfrac{1}{2}(z_0 + z_D) \end{aligned}\right\}, \tag{C.28}$$

are substituted into Eqs. C.21-C.25 to obtain the final equations

$$\left.\frac{\partial(F, r)}{\partial(I, J)}\right|_0 = \tfrac{1}{8}[(F_2 - F_4)(r_A - r_C + r_D - r_B) - (F_1 - F_3)(r_A - r_C + r_B - r_D)], \tag{C.29}$$

$$\left.\frac{\partial(F, z)}{\partial(I, J)}\right|_0 = \tfrac{1}{8}[(F_2 - F_4)(z_A - z_C + z_D - z_B) - (F_1 - F_3)(z_A - z_C + z_B - z_D)], \tag{C.30}$$

$$A_0 = \tfrac{1}{8}[(r_B - r_D)(z_A - z_C) - (r_A - r_C)(z_B - z_D)], \tag{C.31}$$

$$\left.\frac{\partial F}{\partial r}\right|_0 = \frac{1}{8A_0}[(F_2 - F_4)(z_A - z_C + z_D - z_B) - (F_1 - F_3)(z_A - z_C + z_B - z_D)], \tag{C.32}$$

and

$$\left.\frac{\partial F}{\partial z}\right|_0 = -\frac{1}{8A_0}[(F_2 - F_4)(r_A - r_C + r_D - r_B) - (F_1 - F_3)(r_A - r_C + r_B - r_D)]. \tag{C.33}$$

3. Green's Transformation

Green's Theorem in two dimensions is

$$\oint_C F n_i \, ds = \int_A F_{,i} \, dA \tag{C.34}$$

where

n_i = outward normal vector to the surface dA,

C = circuit enclosing the area A,

and

, = covariant differentiation.

In component form, two equations are obtained:

$$\left(\frac{\partial F}{\partial r}\right)_{avg} A = \oint_C F \, dr = \int_A \frac{\partial F}{\partial r} \, dA, \tag{C.35}$$

and

$$\left(\frac{\partial F}{\partial z}\right)_{avg} A = -\oint_C F \, dz = \int_A \frac{\partial F}{\partial z} \, dA, \tag{C.36}$$

which, on substitution in Eqs. C.29 and C.30, yield

$$\left.\frac{\partial(F, z)}{\partial(I, J)}\right|_0 = \oint_C F \, dr \tag{C.37}$$

and

$$\left.\frac{\partial(F, r)}{\partial(I, J)}\right|_0 = \oint_C F \, dz. \tag{C.38}$$

For example, if we choose the circuit ABCD in the illustration (p. 62) and consider the pressure on side AB to be given by its average, etc., and recognize that path of the circuit is counterclockwise, Eqs. C.37 and C.38 give

$$\left.\frac{\partial(F, z)}{\partial(I, J)}\right|_0 = -[F_1(z_A - z_D) + F_2(z_B - z_A) + F_3(z_C - z_B) + F_4(z_D - z_C)] \quad (C.39)$$

and

$$\left.\frac{\partial(F, r)}{\partial(I, J)}\right|_0 = -[F_1(r_A - r_D) + F_2(r_B - r_A) + F_3(r_C - r_B) + F_4(r_D - r_C)]. \quad (C.40)$$

From Eqs. C.39 and C.40,

$$\left.\frac{\partial F}{\partial r}\right|_0 = -\frac{1}{2A_0}[F_1(z_A - z_D) + F_2(z_B - z_A) + F_3(z_C - z_B) + F_4(z_D - z_C)], \quad (C.41)$$

$$\left.\frac{\partial F}{\partial z}\right|_0 = \frac{1}{2A_0}[F_1(r_A - r_D) + F_2(r_B - r_A) + F_3(r_C - r_B) + F_4(r_D - r_C)], \quad (C.42)$$

and

$$A = 2A_0, \quad (C.43)$$

where A_0 is given by Eq. C.23.

REFERENCES

1. W. Prager and P. G. Hodge, *Theory of Perfectly Plastic Solids*, John Wiley and Sons, Inc., New York (1951).

2. S. Timoshenko, *Theory of Elasticity*, 2nd ed., McGraw-Hill Book Co., Inc., New York (1951).

3. L. W. Morland, *The Propagation of Plane Irrotational Waves through an Elastoplastic Medium*, Phil. Trans. Roy. Soc. London, A251, 341-383 (1959).

4. R. von Mises, *Mechanics of Plastic Deformation of Crystals*, Z. Angew. Math. Mech. *8*, 161-85 (June 1928) in German; English Translation: UCRL Trans. 872(L).

5. A. Nadai, *Theory of Flow and Fracture of Solids*, 2nd ed., McGraw-Hill Book Co., Inc., New York (1950).